PERFORMANCE ANALYSIS OF SURFACE PLASMON RESONANCE BASED OPTICAL FIBER SENSORS

A Dissertation Submitted in partial fulfilment of the requirements for the award of the degree of

Masters of Engineering

In

Electronics and Communication Engineering

Submitted by

Pragya

Roll No. : 801361020

Under the guidance of

Dr. R. S. Kaler

Senior Professor and Deputy Director

Thapar University, Patiala

ELECTRONICS AND COMMUNICATION ENGINEERING DEPARTMENT

THAPAR UNIVERSITY

(Established under the section 3 of UGC Act, 1956)

PATIALA – 147004 (PUNJAB)

CERTIFICATE

I, Pragya, hereby declare that the work which is being presented in the dissertation entitled, **"PERFORMANCE ANALYSIS OF SURFACE PLASMON RESONANCE BASED OPTICAL FIBER SENSORS"** by me in partial fulfillment of the requirement for the award of degree of M.E in Electronics and Communication submitted in Electronics and Communication Engineering Department of Thapar University, Patiala is an authentic record of my own work carried out under the supervision of **Dr. R. S. Kaler**, Senior Professor, ECED.

The matter presented in this dissertation has not been submitted in any other University/Institute for the award of degree.

Date: 18-6-15

Pragya
PRAGYA

ROLL NO. : 801361020

It is certified that the above statement made by the student is correct to the best of my knowledge and belief.

Date: 18-6-15

Dr. R. S. Kaler
Senior Professor & Deputy Director
Thapar University

Countersigned By:-

Dr. Sanjay Sharma
Professor & Head
ECED, Thapar University

Dr. S. S. Bhatia
Dean of Academic Affairs
Thapar University

ACKNOWLEDGEMENT

I would like to express my gratitude to **Dr. R.S. Kaler,** Senior Professor, electronics and communication engineering department, Thapar University, Patiala for his patience guidance and support throughout this report work. I am truly very fortunate to have the opportunity to work with him. He has provided help in technical writing, presentation style and I found this guidance to be extremely valuable.

I am highly grateful to **Dr. Sanjay Sharma**, Head, Department of Electronics and Communication, Thapar University, Patiala, for providing this opportunity to carry out the present work.

I also express my gratitude to **Dr. Amit Kumar Kohli,** P.G. Coordinator, Electronics and Communication Engineering Department, the entire faculty and staff members of Electronics & Communication Engineering department for their unyielding encouragement.

I am greatly indebted to all my friends, who have graciously applied themselves to the task of helping me with ample moral support and valuable suggestion. Finally, I would like to extend my gratitude to all those persons who directly or indirectly helped me in process and contributed toward this work.

Pragya

Pragya

801361020

ABSTRACT

Over the past few decades, researchers have shown immense interest in new technology, named Surface Plasmon Resonance (SPR) which utilizes the fascinating light-matter interaction involved at a metal-dielectric interface. This technology is employed for fast and accurate measurement of various physical, chemical and biochemical parameters. The benefits of the SPR based fiber optic sensor are miniaturization of the probe and its utilization in remote sensing applications that is not achievable with prism based SPR sensor.

The objective of this dissertation is to analyze the performance of SPR based optical fiber sensors and for this purpose Opti-Finite Difference Time Domain (FDTD) software is used which allows the design of different configurations SPR sensors.

First study presents the theoretical investigation on the effect of different mode profiles on the guiding region of SPR based optical fiber sensor having gold coated fiber core. Transmission spectra for different transverse magnetic (TM) modes are also compared with respect to the operating wavelength.

Further this dissertation is focused on the theoretical studies of SPR based fiber optic sensors with different materials for sensitivity enhancement. In another study, theoretical analysis of SPR based fiber optic sensor with tri-layer of ITO-Ag-TiO_2 has been performed. The SPR sensor shows high performance characteristics in comparison of bi-layer (ITO-Au) based SPR sensor. Besides it, minima in transmittance curve also dependent on the thickness of the outer layer as well as on middle metal layer used in sensor design.

Finally, the theoretical analysis has been extended to SPR based fiber optic sensor with TCOs (AZO/GZO). The proposed SPR sensor is observed to have high sensitivity and good response as compared to conventional Au/Ag metal-deposited SPR sensors. The benefits of the proposed SPR based fiber optic sensor are low intrinsic loss, semiconductor-based design, compatibility with standard nanofabrication processes, tunability etc. over the conventional metals based SPR sensors.

TABLE OF CONTENTS

LIST OF ACRONYMS

ATR	Attenuated Total Internal Reflection
AZO	Aluminium Doped Zinc Oxide
DA	Detection Accuracy
EMW	Electro Magnetic Waves
EMI	Electro Magnetic Interference
EW	Evanescent Wave
FDTD	Finite Difference Time Domain
FOM	Figure of Merit
FOS	Fiber Optic Sensor
FWHM	Full Width at Half Minimum
GZO	Gallium Doped Zinc Oxide
ITO	Indium Tin Oxide
LED	Light Emitting Diode
LSPR	Localized Surface Plasmon Resonance
MMF	Multi Mode Optical Fiber
MSPW	Multilayer Surface Plasmon Waveguide
NA	Numerical Aperture
NIR	Near Infrared Region
PCF	Photonic Crystal Fiber
RF	Radio Frequency
RI	Refractive Index
RIU	Refractive Index Unit
SERS	Surface Enhanced Raman Scattering
SNR	Signal to Noise Ratio
SMF	Single Mode Optical Fiber
SP	Surface Plasmon
SPR	Surface Plasmon Resonance
SPW	Surface Plasmon Wave

TCO	Transparent Conducting Oxide
TE	Transverse Electric
TIR	Total Internal Reflection
TM	Transverse Magnetic
XPS	X-ray Photoelectron Spectroscopy

LIST OF FIGURES

LIST OF TABLES

CHAPTER 1

INTRODUCTION

1.1 INTRODUCTION

The fiber optic communication industries have witnessed the exponential growth during past few decades. Fiber optics has modernized the telecommunication industry due to its high performance and reliability. The optical fiber are remarkably used for sensing application because they are flexible, light weighted, provides terrific large bandwidth, data multiplexing and small in size. They can also be used in hazardous areas as they are purely dielectric [1]. They are immune to EMI (electromagnetic interference). Further, distributed sensing as well as remote sensing can easily be accomplished by utilising optical fibers. Fiber optic sensors are widely used as a sensing device for physical, chemical and biomedical applications (such as flow, temperature, pressure, rotation, vibration, humidity, refractive index, strain, measurement of concentrations of gases, viscosity and pH etc.) [2]. In fiber optic sensor the light is taken to a modulation region through optical fiber cable, here fiber itself act as a modulator that modulates the incoming light which gives rise to a change in the characteristics like wavelength, intensity, polarization etc. of the guided light, according to the measurand (sample) which is placed in contact with core of the optical fiber and modulated light is received at the detector [3]. The above explained phenomenon is revealed in the figure 1.1 mentioned below:

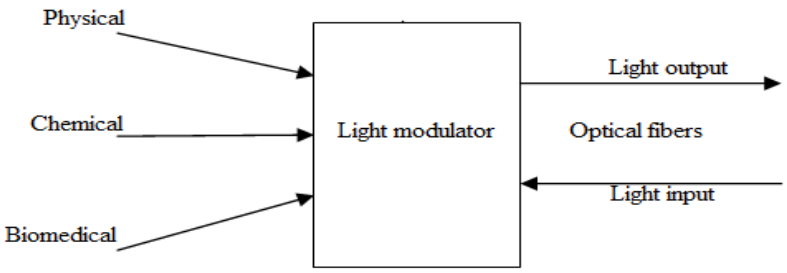

Fig.1.1 Working Principle of the Optical Fiber Sensor

1.2 TYPES OF FIBER OPTIC SENSOR

Fiber optic sensors are primarily classified in three main categories, as shown in fig 1.2 [4]. Based on sensing location, there are two types of sensor, mentioned below:

- **Intrinsic type fiber optic sensors**
  In Intrinsic FOS, the optical fiber itself modulates the light signal according to environmental changes.
- **Extrinsic type fiber optic sensors**
  In Extrinsic FOS, optical fiber does not play any role in sensing. In this type, it is only used for transmission and reception of light.

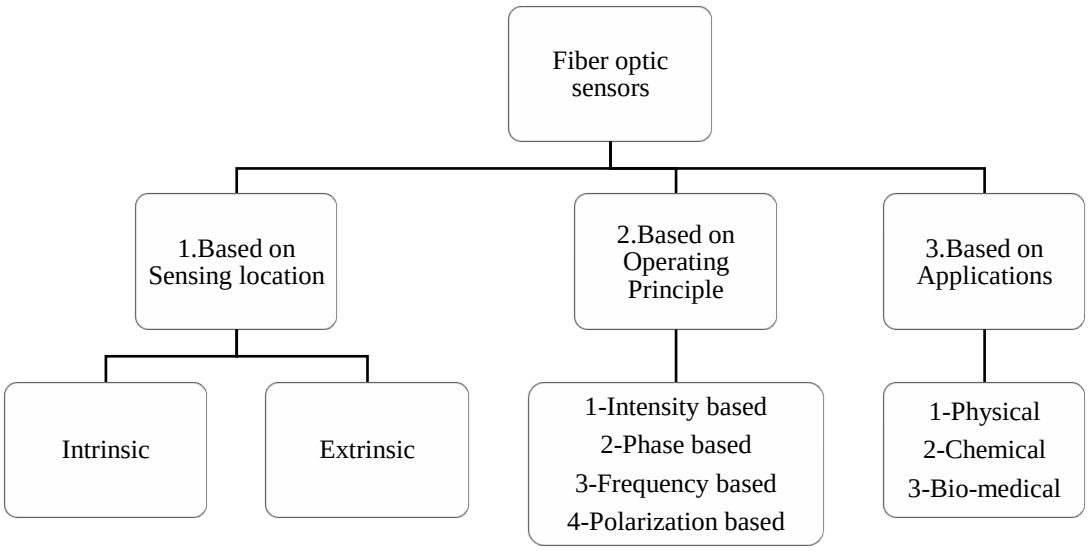

Fig.1.2 Types of the Fiber Optic Sensor

In optical fiber sensors based on operating principle, light intensity, phase, frequency and polarization will work as sensing parameter. Optical fiber sensors has many limitations due to multiple losses in the system that are occurring primarily due to: connections at joints, bending losses (macro, micro) [4].

1.3 SURFACE PLASMON RESONANCE (SPR) BASED FIBER OPTIC SENSORS

There are several optical methods used for sensing purpose like Doppler-effect, interferometry, SPR etc. Apart from all other techniques, SPR has achieved much attention during last thirty years and emerged as a powerful detection technique for various applications like life science, chemical vapour detection, electrochemistry, environmental safety and food [5]. In SPR the desired value is obtained by computing the absorbance, refractive index, and fluorescence properties of measured parameter.

Starting with the first application of SPR [6], several other research groups have used the phenomenon of SPR for sensing various chemical and physical parameters. Except for sensing, SPR technique is also appropriate for miniaturized plasmonic waveguides, microscopic imaging, Surface Enhanced Raman Scattering (SERS) spectroscopy and polarizers.

Surface plasmon process firstly observed by Wood in 1902 [7], he described the occurrence of anomalous diffraction on diffraction grating due to the excitation of SPW. Post which Zenneck determined a surface wave solution to Maxwell's equations and mentioned that the RF surface EMW emerge at the boundary of two media where the first one is loss-free medium and the second one is a lossy dielectric or metal [8]. In 1909, Somerfield described that the field amplitudes of surface waves varied inversely as the square root of the distance from source dipole [9]. In 1957, the SP excitation at a metal surface is theoretically given by Ritchie [10]. In 1968, optical excitation of SPs by the means of ATR is given by Otto and after that modified by Kretschmann in 1971 [11, 12]. However the prism based SPR sensor proposed by Kretschmann has few disadvantages like bulky size, difficulty in optimisation due to presence of different mechanical and optical parts, and are not suitable for remote sensing purpose. SPR based FOS has overcome all above limitations due to its miniaturized structure which makes it suitable for remote sensing as well.

In a SPR based FOS, the metal layer is directly coated on to the fiber core. The SPR sensing process of fixed range of angle of incidence and modulated wavelength is generally used in SPR based FOS. This technique is called wavelength interrogation method. This is because of the reason that spectral distribution of light may be

confined in an optical fiber, while the angular intensity distribution of light will be impossible to differentiate due to mode mixing (as a consequence of inherent bending) of the MMF in sensing applications. Also the sensor is generally fabricated on a MMF, where the angle of incidence is not fixed in fact propagation of light occurs through a range of incident angles [5].

1.4 PLASMONS AND SURFACE PLASMONS

The free electrons in the metal are like electron gas having high density of about 10^{23} cm^{-3}. The positive ions have infinitely large mass in comparison to the mass of the free electrons. As described in Jellium model [13], a positive constant background charge can replace these positive ions. Still, the overall charge density in the conductor stays at zero. Free electrons density is decreased locally, when external electric field is applied on the conductor, as a result, the free electron may start moving and the negatively charged free electrons start getting attracted towards the positive ion background. Hence, free electrons start moving towards the positive region and get accumulated with a density higher than required for the local charge neutrality. At this moment, the Coulomb repulsion acts as a restoring force among the moving free electrons and generates movement in the direction opposite to them. The resultant of these two forces (repulsive restoring force and attractive driving force) produces longitudinal oscillations among the free electrons. These longitudinal density fluctuations are called as plasma oscillations and these oscillations propagate through the entire volume of the metal.

Frequency of plasma oscillations (ω_p) is given by,

$$\omega_p = \sqrt{\frac{4\pi n e^2}{m_0}} \tag{1.1}$$

n = density of free electrons, e = electronic charge and m_0= mass of electron [14]

The coherent oscillations of free electrons or propagation of electron density waves on metal-dielectric interface are called as SPs. They are TM polarized in nature and their excitation is only possible by the TM polarized light. Let us consider a metal and a

dielectric layer to be stacked along the x-axis and the direction of propagation of the surface plasmon wave along z-axis.

The field associated with the surface plasmon wave is given as,

$$E = E_0 \exp\left[i(k_z z \pm k_x x - \omega t)\right] \tag{1.2}$$

+ and – sign are for $x \geq 0$ and $x \leq 0$ respectively. The propagation constant k_x is imaginary resulting the exponential decay of the field. The wave vector k_z is parallel to z-axis and is given as, $k_z = \frac{2\pi}{\lambda_p}$; λ_p is known as plasma wavelength [14]. By applying boundary conditions on the metal-dielectric (M/D) interface, the dispersion relation for surface plasmon wave can be written as [14]:

$$k_{sp} = k_z = \frac{\omega}{c}\sqrt{\frac{\epsilon_m \epsilon_d}{\epsilon_m + \epsilon_d}} \tag{1.3}$$

Where k_{sp} denotes the propagation constant of SPW. ϵ_d and ϵ_m are the dielectric constants for the dielectric and metal respectively, ω represents incident light frequency and speed of light in vacuum is represented by c.

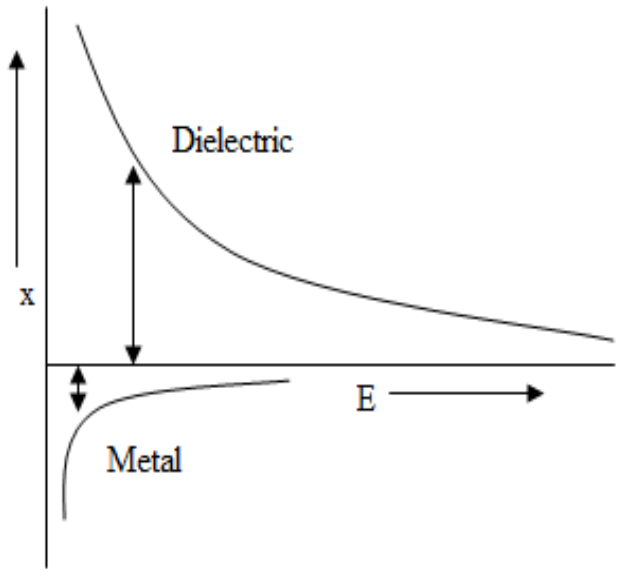

Fig.1.3 Variation of Electric Field Intensity

The exponential decay of the electric field associated with surface plasmon wave across the interface is shown in the fig.1.3.

1.4.1 Propagation Length

Surface Plasmon wave (SPW) is an exponentially decaying wave both in metal as well as in dielectric medium. The dielectric constant of metal $\in_m$ is a complex number and hence from eq. (1.3) the propagation constant of SPW k_{sp} will also be a complex number.

$$k_{sp} = k_z = k_z^{'} + k_z^{"} \tag{1.4}$$

$$k_z' = \frac{\omega}{c}\left(\sqrt{\frac{\epsilon_m' \epsilon_d}{\epsilon_m' + \epsilon_d}}\right) \tag{1.5}$$

$$k_z^{"} = \frac{\omega}{c}\left(\sqrt{\frac{\epsilon_m' \epsilon_d}{\epsilon_m' + \epsilon_d}}\right)\left(\frac{\epsilon_m^{"}}{2(\epsilon_m')^2}\right) \tag{1.6}$$

Where $\in_m = \epsilon_m' + i\ \epsilon_m^{"}$ is the dielectric constant of metal with ϵ_m' as real part and $\epsilon_m^{"}$ as imaginary part [14]. Similarly k_z' is real part and $k_z^{"}$ is imaginary part of propagation constant of SPW. The distance over which the overall intensity of SPW reduces to $1/e$ of its maximum value is known as propagation length and is given as,

$$L_{sp} = 1/(2k_z^{"}) \tag{1.7}$$

For Silver-Air interface at λ=514.5 nm, L_{sp} = 22 μm. L_{sp} becomes 500 μm at λ=1060 nm [14].

1.5 EXCITATION OF SURFACE PLASMONS

There are various methods to excite surface plasmon waves such as: Prism coupling, Grating coupling, excitation using highly focussed optical beams etc. Mostly, the prism coupling is utilized for the excitation of surface plasmon wave. The two different configurations, Otto and Kretschman-Reather configuration are based on prism coupling using the attenuated total internal reflection [12].

1.5.1 Excitation of Surface Plasmon using light

The constant of propagation for light wave (k_{inc}) having frequency ω, in air is represented as:

$$k_{inc} = \frac{\omega}{c} \tag{1.8}$$

For excitation of SPs, the constant of propagation of the SPW and of incident light should be equal. As the SPW is TM polarized, so its excitation is only possible by the p-polarized incident light. As the dielectric constant of dielectric medium is positive and that of metal is negative, hence at a given frequency, the propagation constant of the SPW is always more than k_{inc}. That means SPs can never be excited only by the direct light. Now for exciting the surface plasmon wave at a particular wavelength, an extra amount of momentum is needed. Numerous techniques were utilized to increase the momentum of the light for the excitation of SPs. The effort of increasing this momentum was first made by Otto in 1968 and later this was modified by Kretschmann and Raether [11,12], because the first method was hard to implement practically. These different techniques are discussed below in detail.

1.5.2 Otto Configuration

In 1968, Otto used a coupling prism for the excitation of the SPW [11]. The thought behind the design was the coupling of SPW with the EW, which arises at the bottom surface of a coupling prism due to ATR while beam of light is incident at an angle higher than critical angle (θ_{ATR}) of the interface, as shown in fig.1.4.

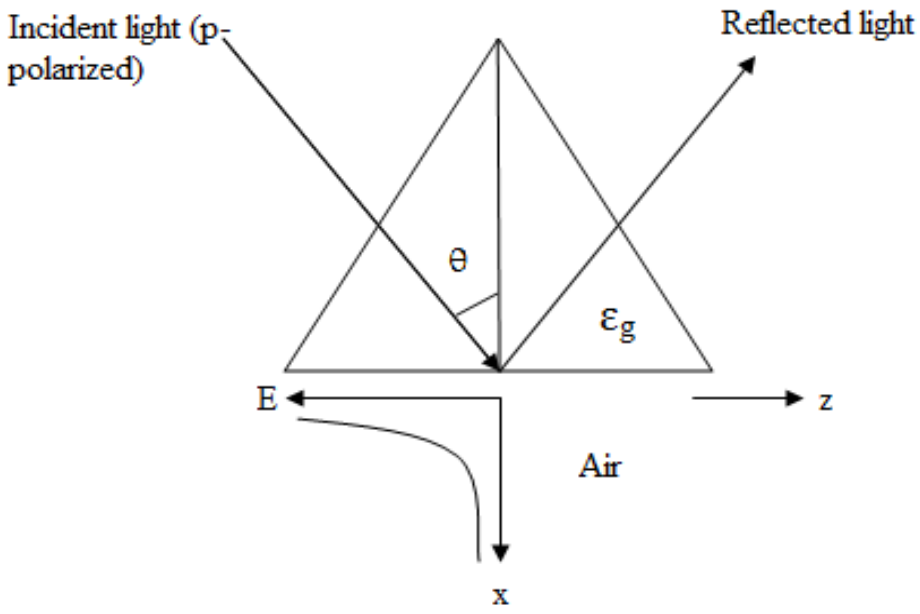

Fig.1.4 Configuration of an evanescent wave at the prism- air interface at an angle $\theta > \theta_{ATR}$

The evanescent wave is decaying in nature and it has the propagation constant along the interface. Both these characteristics of an evanescent wave match to those of a SPW and hence there is a greater opportunity of interaction between these two waves. At prism-air interface, the z-component of the propagation constant of the EW, k_{ev} is specified as:

$$k_{ev} = \frac{\omega}{c}\sqrt{\epsilon_g}\, sin\,\theta \tag{1.9}$$

where dielectric constant of the prism material is ϵ_g and θ is the angle of incident [14].

To excite the SPW in Otto configuration, metal layer is kept below the prism base keeping the gap between the two, as shown in fig.1.5. This gap is filled with the sample having the RI smaller than that of prism. When the wave vectors of SPW and EW are same, the EW excites the SPW at the M/D interface.

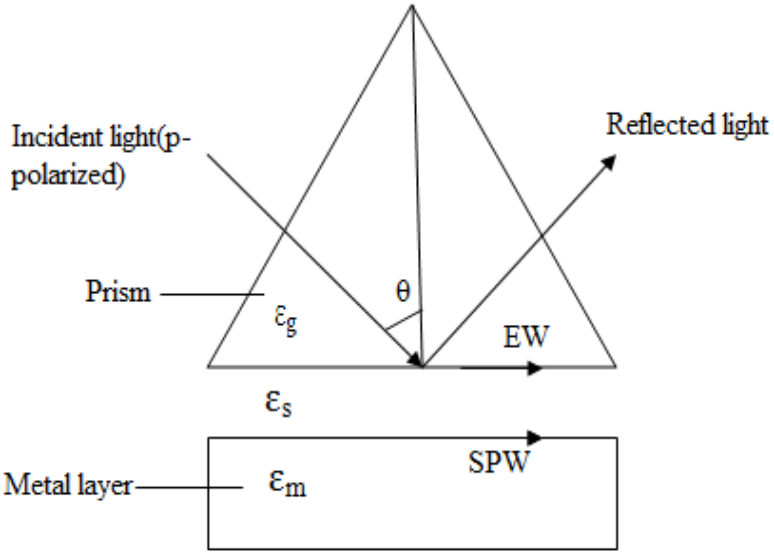

Fig.1.5 Otto configuration for the SPs excitation at M/D interface

When the two wave vectors match, the reflected light shows a minimum. Although, this setup is quite complex to realize as one has to maintain the finite gap between the base of the prism and metal layer.

1.5.3 Kretschmann-Raether Configuration

Like Otto configuration, in this configuration evanescent wave excites the surface plasmons, however here a thin metal film of thickness nearly 50 nm is coated at the base glass prism and placed in contact directly with dielectric sensing medium as shown in fig.1.6 [12]. When p-polarized light is incident through the prism on the interface of the prism-metal layer at an angle $\theta \geq \theta_{ATR}$, the EW is created at prism-metal interface, which propagates along the interface. When the wave vector of EW matches with wave vector SPW, resonance occurs and the energy gets coupled to the surface plasmons. This resonance condition appears as minima in the reflected light intensity. The wave vector (k_{ev}) of the EW is equal to the lateral component of the incident light wave vector (k_g) travelling in the prism [14]. Therefore,

$$k_{ev} = k_g \sin\theta = \frac{\omega}{c}\sqrt{\epsilon_g}\ \sin\theta \tag{1.10}$$

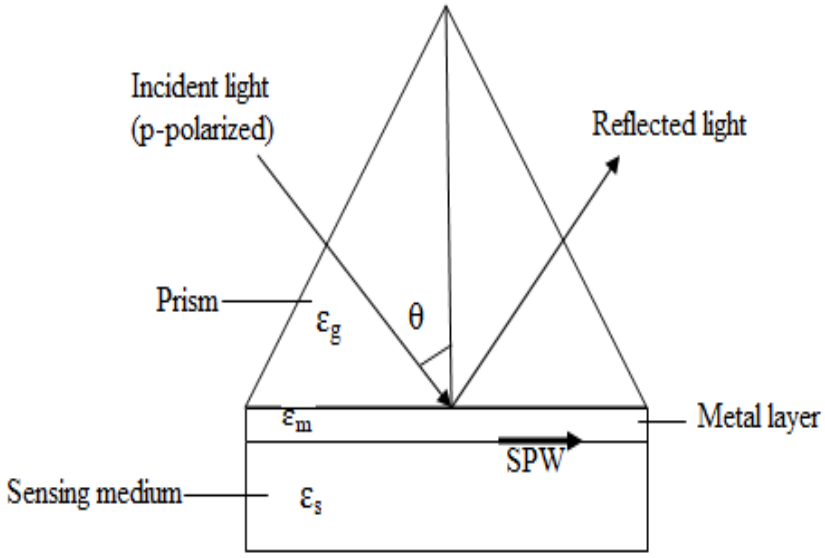

Fig.1.6 Kretschmann configuration for the SPs excitation

The wave vector of the SPW is given by eq.(1.3). As discussed previously, the excitation of SPs takes place only when the wave vector of the SPW matches with wave vector of EW. It happens at a particular incident angle θ_{res} known as resonance angle. This resonance condition is mentioned below:

$$\frac{\omega}{c}\sqrt{\epsilon_g}\,\sin\theta_{res} = \frac{\omega}{c}\sqrt{\frac{\epsilon_m \epsilon_s}{\epsilon_m + \epsilon_s}} \tag{1.11}$$

where ϵ_s is defined as the dielectric constant of the sensing medium.

1.6 SENSING PRINCIPLE OF SPR

The energy transferred from incident light to SPs occurs due to the excitation of SPs at M/D interface. This decreases the reflected light intensity (Reflectance or R) at a specific wavelength known as resonance wavelength and a sharp dip occurs at this specific wavelength. This method is known as spectral interrogation (wavelength interrogation) method, in which light wavelength is varied by keeping the incident angle fixed

However there is another method called as the angular interrogation method, in which the dielectric constant of the medium used for sensing is obtained by changing the

incidence angle but keeping the wavelength fixed. Thus, the RI of the sensing medium can be analysed with the help of resonance wavelength or resonance angle. To cover a greater range of the RI of the sensing medium, the spectral interrogation method is much better [15].

1.7 KRETSCHMANN-RAETHER CONFIGURATION IN OPTICAL FIBER

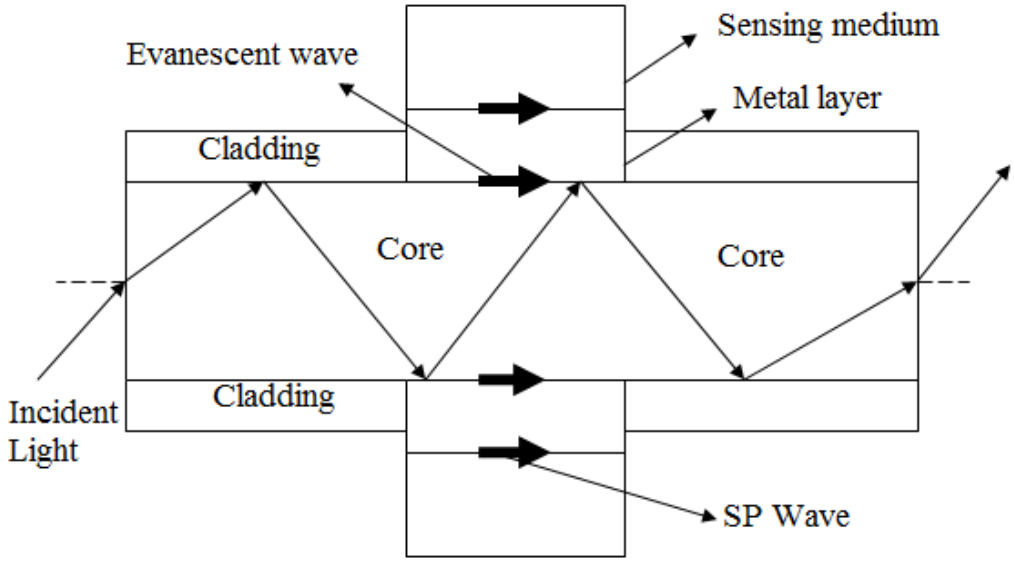

Fig.1.7 Layout of an SPR based optical fiber sensor

In a typical optical fiber, guidance of light takes place through TIR phenomena at the core-cladding interface. An EW is generated in the fiber cladding, which propagates along the core-cladding interface. This evanescent field decays exponentially in the cladding region. Because of these properties, the bulky prism in Kretschmann configuration can be changed with the fiber core. In the FOS based on SPR as shown in fig.1.7, cladding is firstly removed over the core to firm up sensing region which is covered with thin metal layer and further this portion is covered with sensing medium [16].

The incident light from the broadband source is transmitted at one side of the fiber and sensed at the other side of the fiber. By measuring the resultant resonance

wavelength, the RI and hence the dielectric constant of the sensing medium can be determined.

1.8 PERFORMANCE PARAMETERS OF THE SPR SENSOR

Sensitivity is the main performance parameter of a SPR based FOS. To get a better sensing, the sensitivity should be as high as possible and the sensitivity is dependent on the shift in resonance wavelength (wavelength interrogation) or in resonance angle (angular interrogation) with a variation in the RI of the sensing medium. Greater the shift, more will be the sensitivity of the SPR sensor. The resonance wavelength is shifted by an amount $\delta\lambda_{res}$, with increase in RI of the sensing medium by δn_s. Hence, sensitivity is represented as [17]

$$S_n = \frac{\delta\lambda_{res}}{\delta n_s} \tag{1.12}$$

The DA of a sensor is given as the inverse of FWHM of the transmission dip and figure of merit (FOM) is a measure of both of these characteristics, which is defined as [18]

$$\text{FOM} = \text{Sensitivity/ FWHM} = \text{Sensitivity x DA} \tag{1.13}$$

Where, $\text{DA} \propto \frac{1}{\text{FWHM}}$

1.9 OBJECTIVES OF DISSERTATION:

1. To investigate the effect of different mode profiles on the guiding region for various thicknesses of metal layer.

2. To analyse sensitivity of SPR based FOS by using ITO-Ag-TiO_2 coated fiber core.

3. To measure the performance parameters of SPR based FOS by using Transparent Conducting Oxide (AZO/GZO) coated fiber core.

1.10 ORGANIZATION OF DISSERTATION:

This dissertation is divided in six chapters:

Chapter 1 gives general introduction about fiber optic sensors. As the SPR forms the subject of thesis, this chapter covers SPR based fiber optic sensors in detail.

Chapter 2 gives an insight to the topic of dissertation. In order to begin the dissertation, the primary step is to study the papers that have been already published by researchers. With the help of literature review presented, performing this task would get definitely simpler.

Chapter 3 presents the concept of modes for transmittance curve in SPR for different configurations. The various mode profiles are further investigated to examine the impact on the sensitivity of SPR sensor.

Chapter 4 presents the fiber optic sensor based on SPR with tri-layers of oxide-metal-oxide i.e. layers of ITO (as internal layer)- Ag (as center layer)- TiO_2 (as an external layer) coated on fiber core, to improve the sensitivity of sensor.

Chapter 5 explains Transparent Conducting Oxide (TCO)-deposited SPR based FOS with Al:ZnO (AZO) and Ga:ZnO (GZO) coated on fiber core and discuss their suitability for a number of plasmonic applications.

Chapter 6 comprises the Conclusion, Recommendations and Future Scope of the work.

CHAPTER 2

LITERATURE SURVEY

Fiber optic SPR sensor has been an interesting research subject and a number of devices have been reported on fiber optic SPR sensors. However with time, a large number of theoretical and experimental research investigations have been done to improve the sensors performance parameters. The literature survey of the recent SPR based optical fiber sensors for various sensing applications by various researchers in past years is shown below:

Masaru Mitsushio *et al.* [19] (2006) fabricated a metal deposited optical fiber sensors based on SPR consisting Al and Cu having film thickness of 45 nm. The characteristic curves and the various features of these sensors were examined and compared with the SPR sensors having Ag and Au metal films. The optical fiber sensors which use SPR phenomenon with Ag, Au, and Cu metal films have good responses and sensitivities. It was detected that the transmittance spectrums of these sensors with Al, Ag, and Cu demonstrate the impact of the surface oxide layers, which can be seen by using X-ray photoelectron spectroscopy (XPS). A thin oxide layer (approx 0.3 nm) is there on Ag, and thick oxide layers (approx 2 nm) are there on Al and Cu. However the transmittance spectrum of the sensor with Au metal film, computed using theoretical equations of SPR approved significantly with that acquired by the experiment.

The sensor properties of above mentioned metal-deposited SPR based fiber optic sensors depend strongly on the dielectric constants (where ε_r and ε_i are the real and the imaginary parts) of the metal, like:

- Silver (Ag) shows the good response and sensitivity, as it has the high ratio of the constants ($|\varepsilon_r/\varepsilon_i| = 38.0$).
- Copper (Cu) ($|\varepsilon_r/\varepsilon_i| = 20.4$) and Gold (Au) ($|\varepsilon_r/\varepsilon_i| = 7.33$) also shows the good sensor properties but the safety of the copper film from corrosion and oxidation is essential for stability.

- Aluminium (Al) ($|\varepsilon_r/\varepsilon_i|$ = 2.56) has a broader response range and lower sensitivity, so the Al based SPR sensor is helpful for analysing a large range of refractivity. Growth of oxide layer on its surface is self-limiting, so it has stable sensor properties.

Hence it can be concluded that the sensor characteristics of the metal-deposited fiber optic sensor can be managed by the proper choice of the metal film.

Rajneesh K. Verma *et al.* [20] (2008) demonstrated a model for SPR based FOS with three kinds of taper profiles, i.e., parabolic, exponential-linear and linear. The impact of taper profiles and taper ratio on the performance of the sensor is observed and various points are reported as:

- A significant increase in taper ratio is responsible for the increase in sensor's sensitivity.
- The further sensitivity can be improved by utilising the exponential-linear taper profile rather than parabolic or linear taper profile. Thus, to devise a highly sensitive SPR based optical fiber sensor, a large taper ratio and exponential-taper profile can be used.

Masaru Mitsushio *et al.* [21] (2010) investigated the sensor properties and transmittance curves of Al-deposited SPR based FOS having film thickness of 7–70 nm. It can be conclude that

- Al is inexpensive metal and like Ag and Au it is appropriate sensor part for the fiber optic sensor.
- The properties of the said sensor could be managed by thickness of Al film.
- Despite the fact that SPR sensor using Al metal film gives a lesser sensitivity in comparison with Au and Ag film based sensor but is has larger response range, and so the Al based SPR sensor is helpful for analysing a large refractivity range.
- The dense growth of oxide layer on the surface of Al tends to be self limiting, thus it has stable sensor properties i.e. there is no alteration in the properties of sensor after delayed utilization for 5 months.

- The response curve of the sensor with Al metal film, achieved by the experiment matched with the computed response using theoretical equations of SPR.

Tsai Woo-Hu *et al.* [22] (2010) demonstrated a multi-step (with single, two, and three-step) side-polished multi-mode fiber sensor structure to improve the SPR effect, which is based on SPR and TM field-mode coupling phenomena. The said sensor is examined for deionized (DI) water and few points were observed i.e.:

- The proposed sensor structure having the advantages of no complicated signal processing and no bulky components shows an observable SPR response and offers a twice increment in the sensitivity.
- Generally in the first sensing region, the incident TM mode is absorbed and in the coupling region, the TM mode is coupled to the TE mode, which is then utilized for detection in the second region.

Theoretically and the experimentally, it illustrated that with increase in the step number, there is a increase in SPR response.

Sarika Singh *et al.* [23] (2010) theoretically analysed a optical fiber sensor based on SPR with diffuse light source, like LED and study the impacts of core diameter, NA of the fiber, and length of the sensing region on the sensor performance characteristics such as sensitivity, SNR and detection accuracy. The sensor performance using diffuse source has been compared with the performance of the sensor using focusing lens arrangement and collimated light source in the fiber. It has been observed that:

- The performance is fairly better for focusing lens arrangement and collimated source.
- In contrary to this, low cost and miniaturization of the sensor are the beneficial features of the diffuse source based SPR sensor. However the sensor sensitivity can be increased if the fiber with higher numerical aperture, larger core diameter is utilized along with the smaller sensing region length.

Triranjita Srivastava *et al.* [24] (2011) demonstrated a SPR sensor based on high-performance photonic-band gap which deals with the oxidation issue of Al by covering a very-thin layer of gold (Au) on Al and the performance of Al+Au

multilayer surface plasmon waveguide is analyzed with respect to SPR sensor with active metals, for example, aluminum (Al) and gold (Au). It is observed that sensor retains the favourable features of Al based sensor with high sensitivity (5340 nm-RIU^{-1}) and reasonable detection accuracy (130μm^{-1}). The effect on DA and sensitivity of MSPW sensor is very small with respect to substrate. The presented SPR sensor analysis is carried out around 1.50 μm wavelength; so this geometry can be realized in any desired spectral region.

Navneet K. Sharma *et al*. [25] (2012) theoretically and experimentally compared the SPR sensor performance based on four distinct metals, to anticipate the best possible metal for sensing applications.

The experimental results have depicted following points→

- The sensor design consisting of an Al layer shows the deepest SPR dip with the smallest value of resonance wavelength.
- The Cu explains a little wider curve than Al with a higher resonance wavelength.
- Ag also tracks the similar pattern and it has a wider SPR curve and higher resonance wavelength than Al and Cu.
- Au based design gives the widest SPR curve and highest resonance wavelength.

However keeping all the performance characteristics into record, it can be presumed that the SPR based FOS sensor with Au performs better than that designed with other 3 metals. SPR sensors with optimised Au thickness of 50-nm with 10-mm sensing region length, the achieved sensitivity is 2.373 μm-RIU^{-1}.

K. Sathiyamoorthy *et al.* [26] (2013) demonstrated a improved two prism optical arrangement to get better performance of SPR based sensor configurations in chemical and bio analysis. This is a cost effective method that improves the detection sensitivity of surface plasmon by maintaining the surface plasmon (SP) interrogation spot still throughout SPR angular rotation. This arrangement maintains the reflected beam stationary with respect to photodiode and this avoids the use of costly goniometer and linear photodiode that was used in other standard techniques.

Navneet K. Sharma *et al.* [27] (2013) proposed a FOS based on SPR having bi-layers of metal oxide-metal i.e. Au (gold) as outer layer and ITO as inner layer, coated on fiber core and investigated its response curves and sensor properties. For different thickness values of ITO layer i.e. 25, 30, 35nm with 40 nm thick Au layer, the sensitivity of given sensor is theoretically studied. The said sensor has achieved a sensitivity value of 929 nm-RIU^{-1} and 1929 nm-RIU^{-1} for right and left resonance dips respectively. Additionally, an increment in ITO layer thickness diminishes the sensitivity of both right and left resonance dips for all estimations of thickness of Au layer.

Hieu Tu *et al*. [28] (2013) prepared a number of different gold–silver alloy particles, ranging in size from 13 to 34 nm in diameter (nanoparticles) and these particles have been investigated as the active elements of optical fiber sensor systems. This includes a gold-rich group with 25% silver and 75% gold (the A25 group) in content and a silver-rich group with 75% silver and 25% gold in content (the A75 group). Subsequently, the alloy nanoparticles that are synthesized are coated onto the surface of optical fibers to create SPR-based optical fiber sensors for measuring refractive index. The experimental results show that:

- The alloy Size and content also influences the sensitivity of the alloy particle-coated SPR sensors.
- The silver-rich alloy particles (A75) produce a comparatively more sensitive device in term of RI sensing, with (in both the cases of the A25 and A75 groups) the highest sensitivity being demonstrated for the larger particle size.

Priya Bhatia *et al.* [29] (2013) presented an experimental study of SPR based FOS for refractive index sensing, with a high index silicon layer (n-type and p-type) between sensing medium and metal layer (Au and Ag) using the wavelength interrogation method.

- Experimentally, it has been shown that for a specific metal, sensor with n-type silicon has higher sensitivity than p-type silicon based sensor.
- Additionally, the probe coated with Au has greater sensitivity than that coated with silver, for a given type of silicon.

- Numerically, for the silver metal layer the n-type silicon has roughly 1.39 times higher sensitivity than p-type silicon. However the n-type silicon with gold layer has sensitivity roughly 1.50 times higher than the p-type silicon.

As both n-type and p-type silicon have same refractive index, it shows that the majority charge carriers in silicon have a critical contribution in the sensitivity of the SPR based sensor. Therefore it is better to utilize n-type silicon for the improvement of sensitivity.

Yusser Al-Qazwini *et al.* [30] (2014) demonstrated a new bi-layer optical fiber SPR sensor for refractive index measurement, having silver metal layer covered with an over layer of TiO_2. The performance of this proposed sensor structure was compared with bi-metallic layers of Ag and Au in the aqueous media using FDTD method. TiO_2 over layer offers following benefits:

- It greatly improves the sensor performance in terms of SNR and sensitivity compared to that with gold as the over layer.
- It offers the cost effective alternative of gold for overcoming the oxidation problem.
- It also allows tuning the resonance wavelength of SPR sensor, which can broaden its range of applications.

Woo-Hu Tsai *et al*. [31] (2014) presented a SPR sensor based on a side-polished graded-index MMF to enhance the sensitivity of the device, in which an Al:ZnO (AZO)/Au, bi-layer is coated on the side polished surface of fiber core. Bi-layer is utilized as sensing element of the device with a 75nm thick AZO layer over a 40nm thick Au layer. The proposed device is utilized for the measurement of concentration of sodium acetate (CH_3COONa) solutions and results showed that the additional AZO layer may lead to greater measurement stability and higher detection sensitivity in measurement of solution concentration.

H. Moayyed *et al*. [32] (2015) theoretically investigated a double layer SPR based FOS with an internal metallic layer of silver covered with the different oxide materials like titanium dioxide, silicon dioxide, and aluminum oxide. It was shown that the combination of a 50 nm thickness silver inner layer with a dielectric titanium

dioxide layer of a particular thickness gives high-performance phase sensitivity reading.

Akhilesh K. Mishra *et al.* [18] (2015) presented bi-layer SPR based FOS for RI sensing, having silver (Ag) metal layer deposited with over layer of ITO and its response curves and sensor properties is compared with only Ag coated and only ITO coated fiber optic SPR sensor using their respective optimized film thicknesses. A bi-layer sensing structure with a 40-nm thick Ag layer over a 80-nm thick ITO layer is utilized to discover the key parameters of said FOS. It is shown that fiber optic based SPR sensor with ITO+Ag films exhibits a large improvement in detection accuracy and figure of merit for sensing of fluid refractive index and this sensor works in the visible region of spectrum. Apart from being cost effective, the advantages of the proposed SPR sensor are miniaturization of the probe and its utilization in remote sensing that is not possible with prism based SPR sensor.

Table.2.1 Literature survey of fiber optic SPR sensors in past few years.

TYPE	AUTHORS	WORK DONE	RESULTS
Single layer coating on fiber core	Masaru Mitsushio *et al.*	Fabricate the sensor with Al and Cu film	Cu shows the good sensor properties but suffers with oxidation problem. Al has wider response range and lower sensitivity, so it is helpful for analysing a large refractivity range.
	Rajneesh K. Verma *et al.*	Present a theoretical model for SPR sensor with three different taper profiles.	The sensitivity can be improve by using the exponential linear taper profile with high taper ratio instead of using parabolic or linear taper profile.
	Tsai Woo-Hu *et al.*	Using a multi-step side polished multi-mode fiber sensor structure.	There is a increase in SPR response with increase in step number.
	Sarika Singh *et al.*	Theoretically analysed a FOS based on SPR with diffuse light source, like LED.	Low cost and miniaturization are the beneficial features of the diffuse source based fiber optic SPR sensor.
	Navneet K.Sharma *et al.*	Compared the performance of SPR based FOS	Performance of Au deposited FOS was better than that of other

		with four distinct metals: Au,Ag,Cu,Al	three metals based sensor.
	K. Sathiyamoorthy *et al.*	Using a modified two prism optical arrangement.	A cost effective method that improves the detection sensitivity of surface plasmon by keeping the surface plasmon (SP) interrogation spot stationary throughout SPR angular rotation.
Bi-layer coating on fiber core	Priya Bhatia *et al.*	Investigated the SPR sensor with n-type and p-type silicon coated over Ag/ Au metal layer.	It is better to utilize n-type silicon for the improvement of sensitivity of sensor.
	Navneet K. Sharma *et al.*	Proposed a sensor with Au as outer layer and ITO as inner layer, coated on fiber core.	This sensor achieved a sensitivity of 929 nm-RIU^{-1} and 1929 nm-RIU^{-1} for right and left resonance dips respectively.
	Yusser Al-Qazwini *et al.*	Removal of oxidation issue of Ag by covering Ag metal layer covered with over layer of TiO_2.	It greatly improves the sensor performance in terms of SNR and sensitivity compared to that with gold as the over layer.
	Woo-Hu Tsai *et al.*	Designed a sensor with AZO as outer layer and Au as inner layer, coated	AZO layer may lead to greater stability and higher detection sensitivity in

		on fiber core.	measurement of solution concentration.
	Akhilesh K. Mishra *et al.*	Presented a sensor with ITO as outer layer and Ag as inner layer, coated on fiber core.	SPR sensor with ITO+Ag films exhibits a large improvement in detection accuracy and figure of merit for sensing of fluid refractive index and also overcome the oxidation problem of Ag layer.
Multi-layer coating on fiber core	Triranjita Srivastava *et al.*	Performance of Al+Au multilayer surface plasmon waveguide is analysed.	Sensor retains the favourable features with high sensitivity (5340 nm-RIU^{-1}) and reasonable detection accuracy.

CHAPTER 3

EFFECT OF DIFFERENT TM-MODES ON THE SENSITIVITY OF SPR BASED OPTICAL FIBER SENSOR

In this chapter, the SPR based optical fiber sensor (core diameter ≈ 6um) on which a layer of gold metal having thickness (h_{Au}) ≈ 0.5-5 nm is deposited by removing cladding for particular sensing region is analysed. The effect of different mode profiles (TM_{01}, TM_{02}, TM_{03}….TM_{08}) on the guiding region for different thicknesses of metal layer has been examined. The various mode profiles are further investigated to examine the impact on the sensitivity of said sensor. The said mode profiles for above said sensor are studied using finite difference time domain (FDTD) simulations. Transmission spectra for different transverse magnetic (TM) modes are also compared with respect to the operating wavelength. The results show that the thickness of metal film and operating wavelength are responsible for variation in the sensitivity with respect to TM modes of the said sensor.

3.1 INTRODUCTION:

Numerous techniques have been used for sensing, such as Doppler effect, interferometry, photolumnisense and surface plasmon resonance (SPR). Apart from all other sensing techniques, SPR is developed as a dominant detection method in real time with variety of various applications like, life science, chemical vapour detection, electrochemistry, environmental safety and food. In SPR, the desired quantity is determined by computing the RI, absorbance and fluorescence properties of measured parameter [5]. In this technique, when the p-polarised light having propagation constant equivalent to that of surface plasmon wave (an electromagnetic wave supported by metal-dielectric interface) is incident on M/D interface, a strong absorption of light happens, hence SPR causes a decrease in the intensity of light reflected at specific wavelength or angle from the glass side of the sensor surface [16].

Masaru Mitsushio *et al*. [21] investigated the sensor characteristics and response curves of Al-deposited OFS based on SPR, having Al film thicknesses of 7–70 nm. S. Lee *et al.* [33] presented the method for determining the effective indices, field distributions and mode numbers of the guiding modes for planar waveguides. Ruschin *et al.* [34] and J. W. Y. Lit *et al.* [35] both used simplified equations that were transformed from the field-transfer matrix to characterize the mode properties for planer waveguides. Above said study limits the mode profile only to certain parameters. None of them discussed the sensitivity and mode relations. Thereby, for the first time to our knowledge, the effect of different mode profiles (TM_{01}, TM_{02}, TM_{03},….. TM_{08}) on the guiding region for different thicknesses of metal layer is described here. The different mode profiles are further investigated to examine the impact on the sensitivity of said sensor.

This chapter is divided in four sections. In section 2, the simulation setup for comparison of sensor performance with varying parameters, is discussed with component details. Section 3 deals with the detailed discussion of results observed after the simulation. Section 4 gives the conclusion of the dependence of sensor performance with varying parameters.

3.2 THEORY AND SIMULATION SETUP

The principle of SPR sensing is ATR with Kretschmann's setup [12]. FOS based on SPR is presented with fiber core-gold-sensing medium as revealed in fig.3.1. As structure follows, cladding is firstly removed over the core (fiber core diameter = 6 μm and numerical aperture = 0.18) to firm up sensing region which is coated with thin metal layer and further covered with sensing medium. The light from the broadband source is incident at one side of the fiber and the transmitted light is sensed at the other side of the optical fiber.

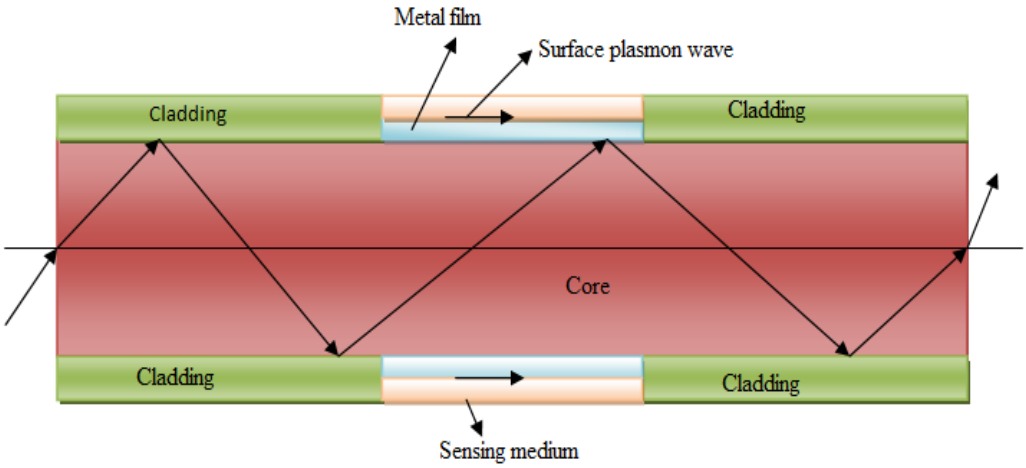

. Fig.3.1 Schematic layout of fiber optic sensor based on SPR

Table 3.1: Parameters utilized for optical fiber:

Parameter	Numerical value
Fiber core diameter (D)	6 µm
Sensing region length (L)	100 µm
Numerical aperture (NA)	0.18

3.2.1 First Layer (Fiber core)

In fig.3.1, the fiber core is considered as first layer. The RI of fused silica (n_1) changes with wavelength, indicated by Sellmeier dispersion relation given as [36]:

$$n_1(\lambda) = \sqrt{1 + \frac{A_1\ \lambda^2}{\lambda^2 - B_1^2} + \frac{A_2\ \lambda^2}{\lambda^2 - B_2^2} + \frac{A_3\ \lambda^2}{\lambda^2 - B_3^2}} \quad (3.1)$$

Where λ = wavelength of incident light in µm with Sellmeier coefficients A_1 =0.6961663, A_2 = 0.4079426, A_3 =0.8974794, B_1=0.0684043µm, B_2= 0.1162414 µm, B_3= 9.896161 µm, with λ=1.55 µm, For λ=1.55um, $n_1(\lambda)$ comes out to be 1.4440.

3.2.2 Second Layer (Gold layer)

Second layer is comprised of Au metal and the dielectric constant of any metal $\in_m$ can be determined by Drude model [37] as,

$$\in_m (\lambda) = \in_{mr} + i \in_{mi} = 1 - \frac{\lambda^2 \lambda_c}{\lambda_p^2 (\lambda_c + i\lambda)} \quad (3.2)$$

Where λ_p = 1.6826 $\times 10^{-7}$m (plasma wavelength) and λ_c = 8.9342$\times 10^{-6}$m (collision wavelength)

3.2.3 Third Layer (Sensing medium)

The Au metal layer is surrounded with sensing medium, with dielectric constant ($\in_s$) which is related to RI of sensing medium n_s, as $\in_s = n_s^2$.

For excitation of SPW, the resonance condition is specified as [15]:

$$\frac{2\pi}{\lambda} n_1 \sin\theta = Re\ \{K_{sp}\} \quad (3.3)$$

where $K_{sp} = \frac{w}{c}\sqrt{\frac{\in_m \in_s}{\in_m + \in_s}}$ is the surface plasmon propagation constant, c is speed of light in vacuum and ω is frequency of incident light. A change in the RI of sensing medium is calculated; by examine the shift in the resonance wavelength.

3.3 MODE THEORY

Modes define the electric field and magnetic field distribution inside the optical fiber. It is considered that light propagates along the 'z' direction and any direction which is perpendicular to 'z' axis is called transverse direction. Let E_z and H_z are two independent longitudinal components and with the help of these components and by using Maxwell's equations, all transverse components can be calculated.

Here, three possibilities of modes are described depending on orientation of E.F. with respect to the plane of incidence.

- If $E_z = 0$, $H_z \neq 0$: TE mode.
- If $E_z \neq 0$, $H_z = 0$: TM mode.
- If $E_z \neq 0$, $H_z \neq 0$: Hybrid mode.

In cylindrical coordinate system(r, ϕ, z) it is considered that Φ (ϕ) = $e^{jv\phi}$, where ν is integer, which indicates the variation of the field with respect to ϕ. If ν = 0, it indicates a circularly symmetrical field in the azimuthal direction with maximum intensity at the centre of fiber and gradually decreasing towards the periphery of core of the fiber. It can also be said that if ν = 0, it corresponds to meridional rays and supports TE and TM modes and if ν > 0, it corresponds to skew rays and it supports Hybrid modes.

The combination (ν, m) helps us to identify a particular mode and its corresponding light intensity pattern. 'ν' represents the number of complete cycles of field in azimuthal plane and 'm' represents the number of zero crossing in azimuthal direction. The number of zero-crossing is one less than the index 'm'. The different modes can be designated as:

- TE_{0m} = TE_{01}, TE_{02}.....
- TM_{0m}= TM_{01}, TM_{02}.....
- HE_{vm} = HE_{12}, HE_{23},…

V-number is one more fundamental and characteristic parameter of an optical fiber, with which the number of guided modes is obtained, and which is proportional to the frequency of the propagating light. That is why it is known as normalized frequency. It does not depend on individual characteristics of the core or the cladding but depends on the characteristics of the combination of the core-cladding.

$$V = \frac{2\pi a}{\lambda}(N.A.) \tag{3.4}$$

$$\text{N.A.} = \sqrt{(n_1^2 - n_2^2)} \tag{3.5}$$

a = radius of the optical fiber

λ = wavelength of light

n_1= RI of core

n_2 = effective RI of cladding

V = 2.4 is the first root of zero order Bessel function. If V number is smaller than 2.4 it signifies SMF, and only one mode, HE_{11} can propagate. If V number is greater than 2.4, it signifies MMF.

When the wave equations are solved by using cylindrical co-ordinate system, it gives the radial variation of electric and magnetic field distribution. Inside the Core, field distribution is oscillatory in nature, which is represented by Bessel functions and inside cladding; field is monotonically decaying in nature, which is represented by modified Bessel functions.

Due to field distribution in core and cladding, the propagation constant β can be written in bounded form like [38].

$\beta_2 < \beta < \beta_1$; where β_1 and β_2 are phase constants of the material of core and cladding respectively.

$\beta_0 n_2 < \beta < \beta_0 n_1$; where β_0 is phase constant of wave in vacuum.

$n_2 < \beta / \beta_0 < n_1$ or

$n_2 < n_{eff} < n_1$

where n_{eff} is effective modal index and n_1 and n_2 are RI of core and cladding of fiber respectively. By considering n_{eff}, transverse magnetic (TM) modes can be calculated.

3.4 RESULTS AND DISCUSSION

In the previous sections, various components used in the simulation setup were discussed. Using this setup the measurement of magnitude of dip in transmittance curve for different cases has been performed. The result discussed below gives the comparison of transmittance curves for all the considered cases.

In fiber optic sensor based on SPR, TM modes are calculated by considering the effective modal index, they can be designated as: TM_{0m}= $TM_{01,}$ TM_{02}.....Mode patterns are related to the variation of light intensity across the plane perpendicular to the direction of propagation and have certain properties such as, the electric field varies across the guiding region; evanescent field which is generated due to surface plasmon resonance decreases exponentially outside the core. Fig.3.2, as shown below describes that 'm' gives the number of zero crossings performed by electric field which is penetrated through guiding region. Low order modes exist which are nearly parallel to the boundary at a given thickness of gold layer h_{Au}, while higher order modes have steep zigzag paths. Higher order modes penetrate deeply into cladding and have much more losses.

The above described properties can easily be seen in the fig.3.2 showing all the 9 TM modes, which are calculated by considering the metal thickness (d_m) of around 0.5 at operating wavelength (λ) 1.55 μm in SPR based optical fiber sensor.

In FDTD simulation, with given thicknesses and effective index of core and cladding, 9 TM modes have been observed with different effective modal indices and which are responsible for the variation of intensity in sensing curve with varying modes and it is being shown that all TM modes can be excited at one observation point i.e., at same resonance wavelength for the given incident angle. However, all TM modes respond to different modal indices, so there is a variation in the magnitude of the dip. The above described properties can easily be seen in the fig.3.3 as shown below.

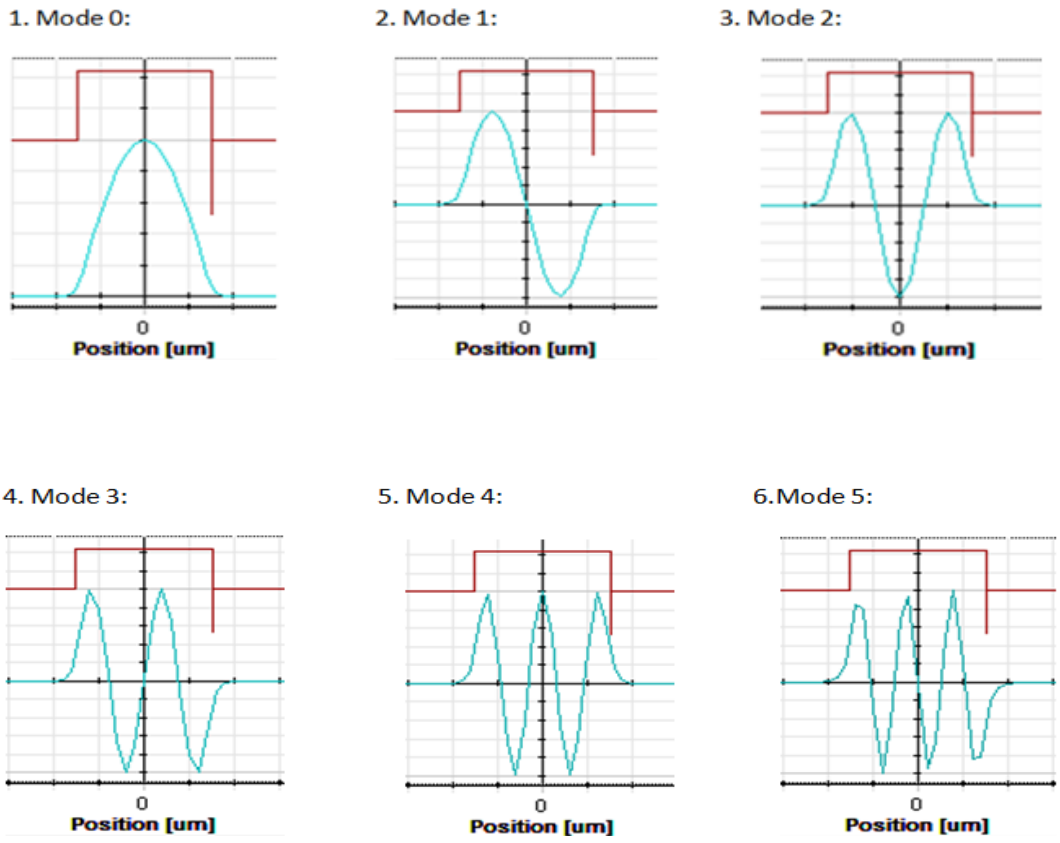

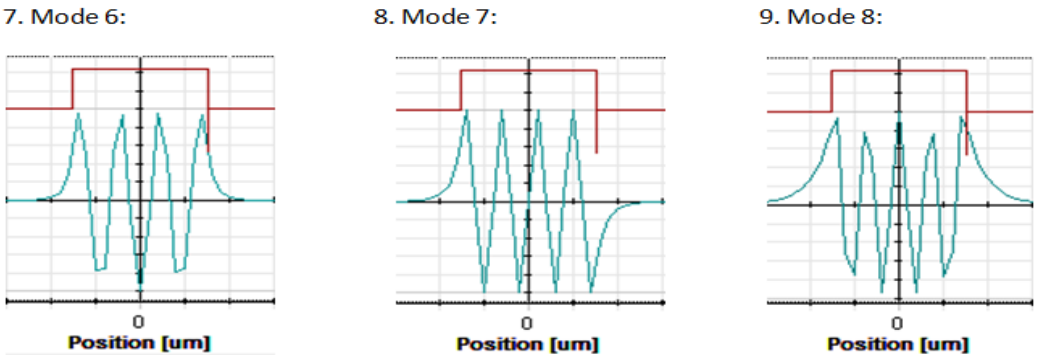

Fig.3.2 Different TM modes generated in SPR based fiber optic sensor

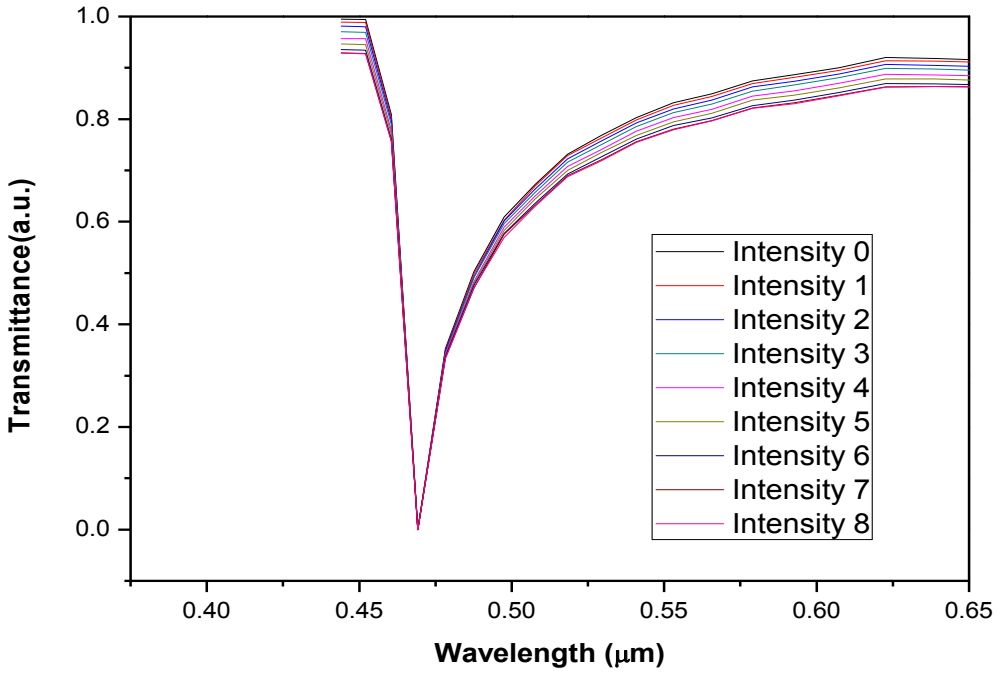

Fig.3.3 Variation of intensity in transmittance curve with all TM modes

The variation of intensities for all 9 TM modes with respect to the wavelength is shown in fig.3.3. These are calculated by considering the metal thickness (d_m) of around 0.5 nm at operating wavelength (λ) 1.55 μm in SPR based fiber optic sensor.

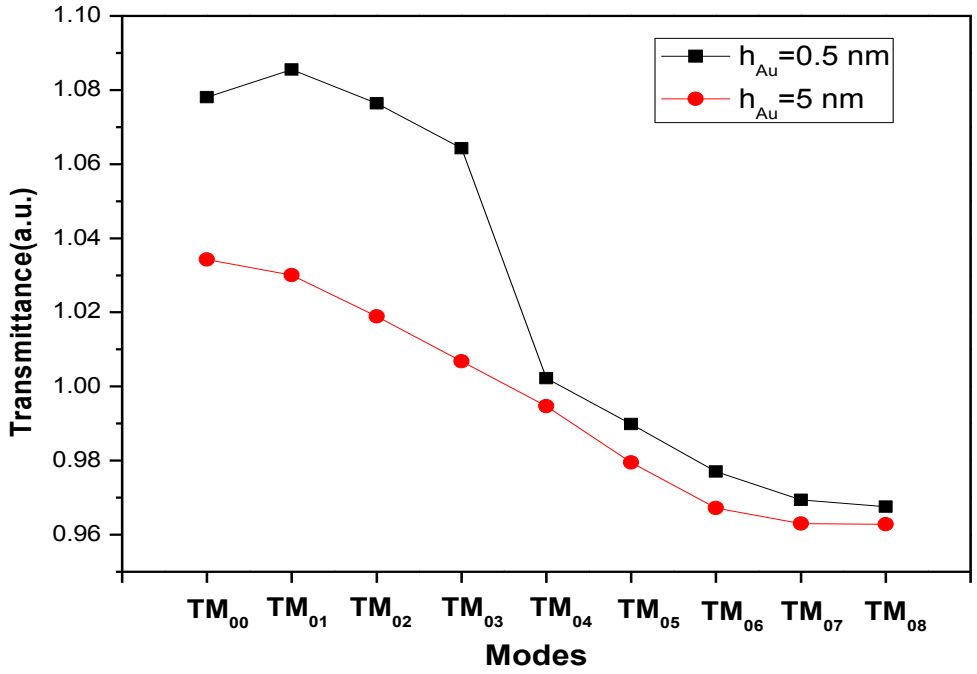

Fig.3.4 Shift in the intensity of transmittance curve for different thicknesses of metal film.

The effect of modes on the SPR-based FOS has been studied with some consideration of thickness of metal layer and operating wavelength. For these generated modes, it has been kept in mind that below this thickness of metal layer h_{Au}, all above said modes will not prevail. We compared the result of transmission spectrum for all 9 TM modes, for metal layer having thickness ($h_{Au} \approx 0.5$-5 nm), as shown in fig.3.4. Further by increasing the thickness of metal film, we analysed 9 TM modes but with different effective modal indices from the optimised thickness of metal film ($h_{Au=}$ 0.5 nm) and which are also responsible for the variation of intensity in sensing curve with varying TM modes. Fig.3.4 also depicts that when we increased the thickness of metal film, the variation in intensity is less than that obtained at optimised thickness.

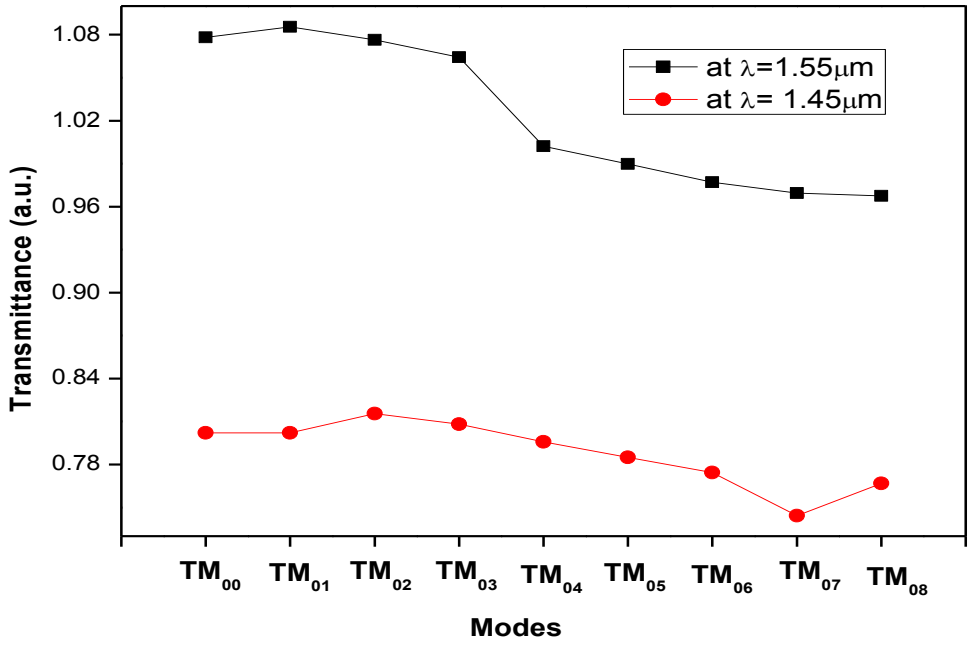

Fig.3.5 Shift in the intensity of transmittance curve for different operating wavelengths

The intensities for all TM modes with respect to the sensitivity for varying operating wavelengths (1.55 μm - 1.45 μm) have been compared and shown in fig.3.5 and it also illustrates that, by decreasing the operating wavelength, still we observed all TM modes but with different effective modal indices from those observed at wavelength of 1.55 μm and which are also responsible for the variation of intensity in sensing curve with varying TM modes.

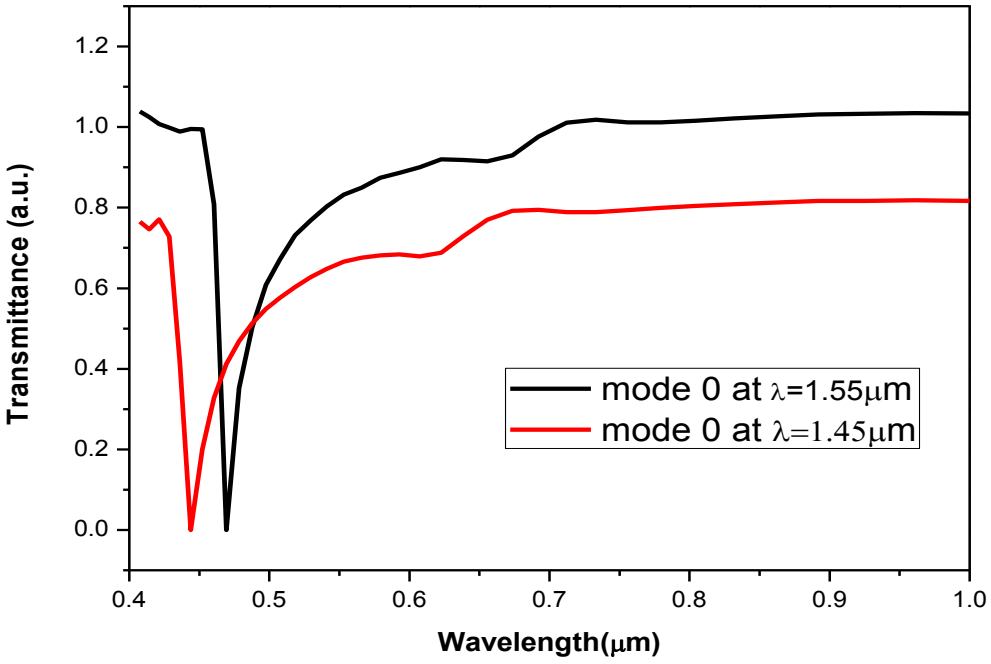

Fig.3.6 Shift in resonance wavelength of sensing curve for gold

Fig.3.6 is describing that at operating wavelength 1.55 μm, the resonance wavelength is equal to 0.4691 μm whereas at operating wavelength 1.45 μm the resonance wavelength is 0.4439 μm. So there is shift of 0.0252 μm in resonance wavelength with different operating wavelengths. This case explains that when we changed the operating wavelength with the given configuration, there is shift in the resonance wavelength with the variation in the magnitude of the dip in transmittance curve with varying modal index.

3.5 CONCLUSION

The concept of modes for transmittance curve in SPR for different configurations has been presented. The various mode profiles are further investigated to examine the impact on the sensitivity of said sensor. All mode profiles for this sensor are studied using finite difference time domain simulations. Transmission spectra for different TM modes, are also compared for different operating wavelengths. We observed that the thickness of metal film and operating wavelength are responsible for variation in the transmittance with respect to TM modes of the said sensor.

CHAPTER 4

WAVELENGTH INTERROGATED FIBER OPTIC SENSOR BASED ON SPR WITH OXIDE-METAL-OXIDE LAYERS USING FDTD SOLUTIONS

In this chapter, a new tri-layer SPR based fiber optic refractive index sensor with ITO-Ag-TiO_2 layers coated on fiber core is presented and analysed theoretically. The optimal thicknesses of each layer in said sensor are numerically examined and the performance characteristics of sensor design are compared with bi-layer (ITO-Au) SPR based fiber optic sensor using FDTD method. The effect of different thicknesses of over layer of TiO_2 on the guiding region of the said sensor for given operating wavelength is also examined. The results show that the tri-layer based SPR sensor possesses higher sensitivity.

4.1 INTRODUCTION

SPR based FOS is widely used in sensing applications as the SPs are highly sensitive to the change in the RI of the surroundings [39]. In SPR, when the p-polarised light having propagation constant equivalent to that of surface plasmon wave (an electromagnetic wave supported by metal-dielectric interface) is incident on M/D interface, a strong absorption of light occurs, hence SPR causes a decrease in the intensity of light reflected at specific angle or wavelength from the glass side of the sensor surface [16].

For sensing applications, noble metal surfaces like silver (Ag)/ Gold (Au) metals are conventionally used to perform SPR because they show free electron behaviour as explained by free electron model [40]. These metals have some preferences over other type of metals; as they show SPR bands in both near-infrared and visible frequencies, and they are effectively functionalized, additionally Au/Ag films are easily arranged by a various deposition methods. [19].

Navneet K. Sharma *et al.* [27] investigated the response spectrum and sensor properties of FOS based on SPR with bi-layers of ITO-Au coated on the fiber-core and achieved a sensitivity value of 929 nm-RIU^{-1} and 1929 nm-RIU^{-1} for right and left resonance dips respectively. A.K. Mishra *et al*. [18] presented a SPR based ITO-Ag coated fiber optic sensing probe for refractive index sensing with enhanced detection accuracy in visible region. Yusser Al-Qazwini *et al*. [30] also presented bi-layer SPR based FOS with Ag as inner layer, coated with an over layer of TiO_2.

Above said study limits the sensor structure only to bi-layers coated on the fiber core and noble metal films experience various drawbacks, like they are mechanically delicate and are effortlessly degraded by handling, they have a tendency to form discrete islands, as opposed to a continuous film, when the film thickness is not lower than the critical value, last is Ag metal films are prone to the oxidation [41]. To overcome the above problems either we can use new materials like transparent conducting oxides, graphene etc [42] or we can use layers of other materials which are called sandwich films. Layers above the SPR-active film can enhance the chemical and mechanical strength and layers below the active film can reduce the start of island development [43].

In this chapter, for the first time to our knowledge, to improve the sensitivity of ITO based SPR sensor, a Tri-layer i.e. ITO-Ag-TiO_2 structure of SPR sensor has been presented. The FDTD method is used to simulate the said sensor for refractive index sensing and spectral interrogation method is utilised to examine the said sensor. Not only this structure has a good sensitivity but also overcomes the disadvantages of noble metal films.

This chapter is divided in four sections. In section 2, the theory and simulation setup for comparison of sensor performance with varying parameters, is discussed with component details. Section 3 deals with the detailed discussion of results observed after the simulation. Section 4 gives the conclusion of the dependence of sensor performance with varying parameters.

4.2 THEORY AND SIMULATION SETUP

ATR with Kretschmann's setup is the principle of SPR sensing [12]. In this chapter, the FOS based on SPR is presented with sandwich films represented as ABC layer structure, where A is a transparent conducting metal oxide layer like ITO, B is the metal layer of Ag and C is an oxide layer of TiO_2 shown in fig.4.1. As structure follows, cladding is firstly removed over the core (fiber core diameter = 20 µm and numerical aperture = 0.24) to firm up sensing region which is coated with ABC sandwich layers and further, covered with sensing medium.

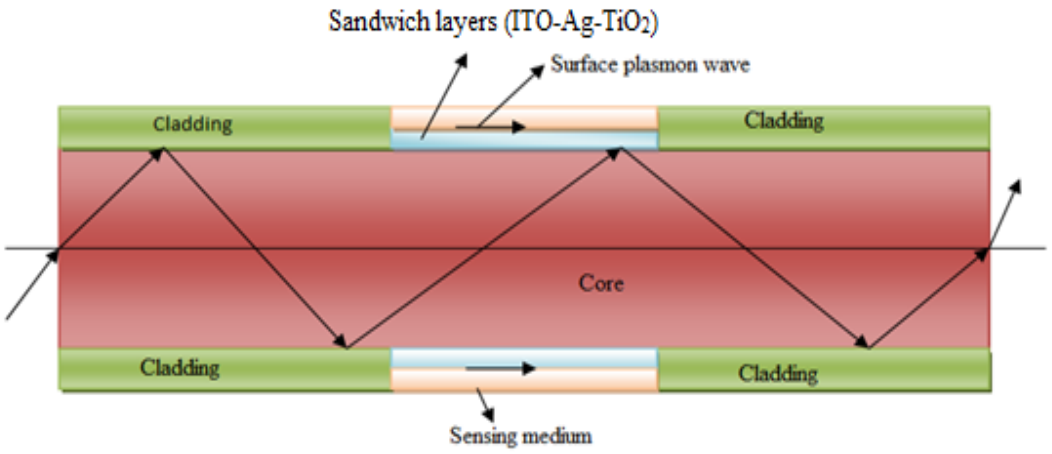

Fig.4.1 Schematic layout of tri-layer SPR based fiber optic sensor.

Table 4.1: Parameters utilised for optical fiber:

Parameter	Numerical value
Fiber core diameter D	20 µm
Numerical aperture (NA)	0.24
Sensing region length L	100 µm

4.2.1 First Layer (Fiber core)

The fiber core made up of fused silica is considered as first layer, as shown in fig.4.1. The wavelength dependency of the RI (n_1) of the fiber core is determined by Sellmeier dispersion relation as given below [36]:

$$n_1(\lambda) = \sqrt{1 + \frac{A_1\ \lambda^2}{\lambda^2 - B_1^2} + \frac{A_2\ \lambda^2}{\lambda^2 - B_2^2} + \frac{A_3\ \lambda^2}{\lambda^2 - B_3^2}} \quad (4.1)$$

Where λ = wavelength of incident light in μm with Sellmeier coefficients A_1 = 0.6961663, A_2 =0.4079426, A_3 =0.8974794, B_1=0.0684043μm, B_2= 0.1162414μm, B_3= 9.896161μm.

4.2.2 Second Layer (ITO layer)

Surface plasmon resonance can be achieved with (TCO) transparent conducting metal oxide thin film. Our first choice for TCO is Sn doped In_2O_3 i.e. indium tin oxide (ITO) since for generation of surface plasmons, ITO is considered as a good alternative of noble metals (Ag and Au) [41]. ITO is most privileged because it offers maximum available transmissivity for visible light with least electrical resistivity [44]. Carrier concentration of extremely conductive ITO materials generally lies in the range of 10^{20} to 10^{21} cm^{-3}. In addition, thin layers of ITO are continuous (i.e. no agglomeration as islands) and no contribution of band to band transitions [45]. So second layer is comprised of ITO and its dielectric constant can be given by the Drude model as [42],

$$\epsilon_m(\lambda) = \epsilon_{mr} + i\,\epsilon_{mi} = 3.8 - \frac{\lambda^2 \lambda_c}{\lambda_p^2(\lambda_c + i\lambda)} \quad (4.2)$$

Here, λ_c and λ_p are the collision wavelength and the plasma wavelength. Where, λ_p = 5.649 x 10^{-7} m and λ_c = 11.121 x 10^{-6} m for ITO respectively.

4.2.3 Third Layer (Ag layer)

Third layer is comprised of Ag metal, as SPR sensors with a thin layer of Ag exhibit an improvement in the sensitivity and detection accuracy compared to those with Au [40], because silver has the largest $|\frac{\epsilon_{mr}}{\epsilon_{mi}}|$ ratio, where ϵ_{mr} and ϵ_{mi} are the real and imaginary parts of the dielectric constant, that are responsible for the reflection and absorption of light in the metal, respectively [46]. The Drude model has been used for calculating the dielectric constant of Ag metal as given below: [37]

$$\epsilon_m(\lambda) = \epsilon_{mr} + i\,\epsilon_{mi} = 1 - \frac{\lambda^2\lambda_c}{\lambda_p^2(\lambda_c + i\lambda)} \quad (4.3)$$

Where $\lambda_p = 0.14541\times10^{-6}$m (plasma-wavelength) and $\lambda_c = 17.6140\times10^{-6}$m (collision wavelength).

4.2.4 Fourth Layer (TiO_2 layer)

SPR sensor using Ag metal as outer layer is not chemically stable because of the fact that Ag is extremely prone to oxidation. This issue of Ag layer is wiped out by covering another layer on it. An alternative for the protection of SPR metallic layer is oxides over layers, due to their low cost and good chemical stability [47]. The addition of oxide over-layers of high refractive indices such as titanium dioxide (TiO_2) extends the local Electric-field intensity at the interface between the oxide over-layer and sensing medium. An increase in the E-field intensity results in an increase in the shift in the SPR wavelength with the varying RI of the sensing medium which will improve the sensitivity [48].

Fourth layer is made up of TiO_2 and the wavelength dependent RI of TiO_2 can be written by following expression [49] as,

$$n_{TiO_2}(\lambda) = \sqrt{5.913 + \frac{0.2441}{\lambda^2 - 0.0843}} \quad (4.4)$$

4.2.5 Fifth Layer (Sensing medium)

The TiO_2 layer is surrounded with sensing medium, with dielectric constant ϵ_s ,which is related to RI of sensing medium ns, as $\epsilon_s = n_s^2$. Here, n_s is varied from 1.443 to 1.444. A change in the RI of sensing medium can be measured, by examining the shift in the resonance wavelength.

4.3 RESULTS AND DISCUSSION

In the previous sections, we discussed various components used in the simulation setup. Using this setup the measurement of magnitude of dip in transmittance curve for different cases has been performed. The result discussed below gives the comparison of transmittance curves for all the considered cases.

The transmission spectrum shows a minima at a specific wavelength; recognized as resonance wavelength (λ_{res}).The change in RI of sensing medium leads to change in λ_{res}, which is the basic concept of RI sensing. The SPR sensor response was plotted as normalized transmitted power (i.e., to the source power) versus wavelength, as shown in fig.4.2 and we analysed that resonance wavelength is shifted towards the lower value with increase in the refractive index.

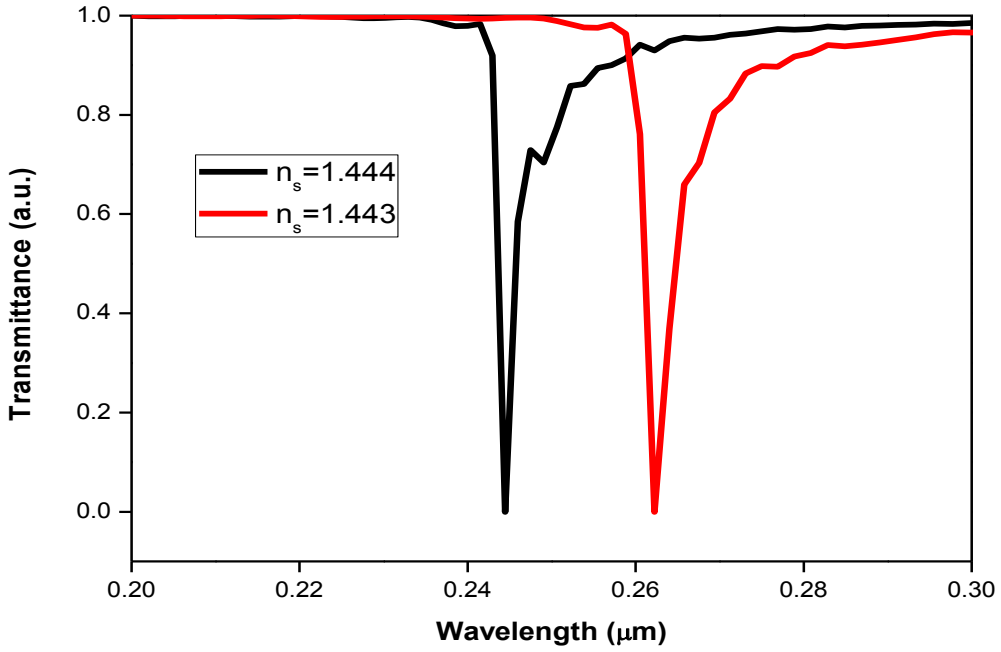

Fig.4.2 Shift in resonance wavelength of sensing curve for gold

The sensor performance is measured in terms of two attributes: sensitivity (S_n) and DA. When the resonance wavelength is shifted by an amount $\delta\lambda_{res}$ with increase in RI of the sensing medium by δn_s then sensitivity of sensor is characterized as: $S_n = \frac{\delta\lambda_{res}}{\delta n_s}$. DA decides the precision of measurement of λ_{res} and is characterized as DA = $1/\Delta\lambda$, where $\Delta\lambda$ is FWHM of the transmittance curve. A high performance sensor must have high value of S_n and DA [24].

For estimating the sensor performance of said sensor, we calculated S_n = 17,807 nm-RIU^{-1} and DA = 0.5263 nm^{-1} from fig.4.2.

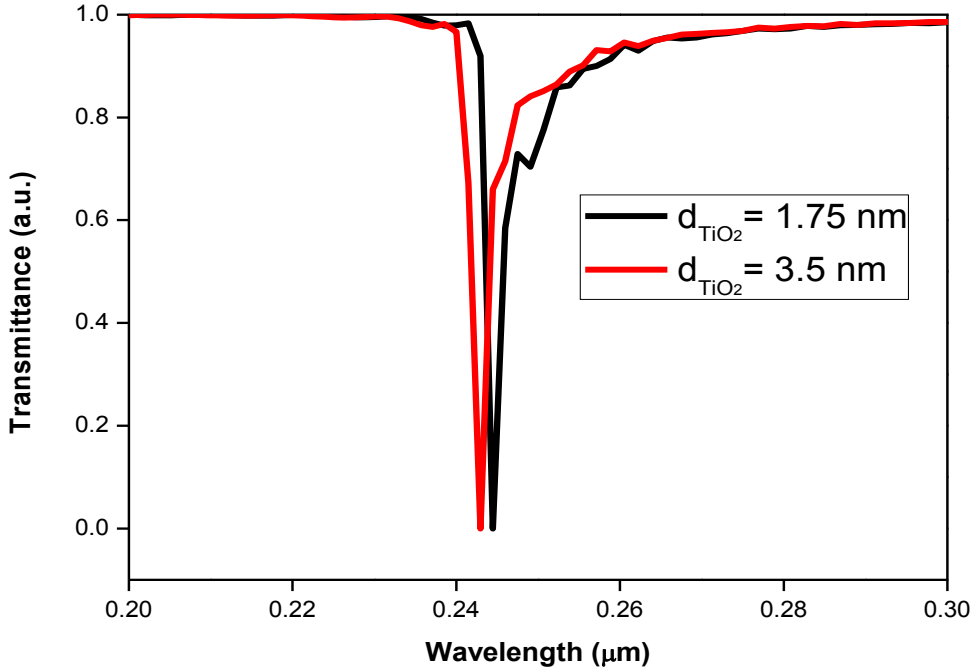

Fig.4.3 Variation of λ_{res} as a function of TiO_2 layer thickness

The shift in resonance wavelength in transmittance curve of said sensor for different thickness values of TiO_2 layer i.e. 1.75 nm, and 3.5 nm with fixed 10 nm ITO and 3.5 nm Ag layer, have been plotted in fig.4.3. The resonance wavelength is observed at 0.24444 μm for d_{TiO_2}=1.75nm and is shifted to 0.24294 μm for d_{TiO_2}=3.5 nm.

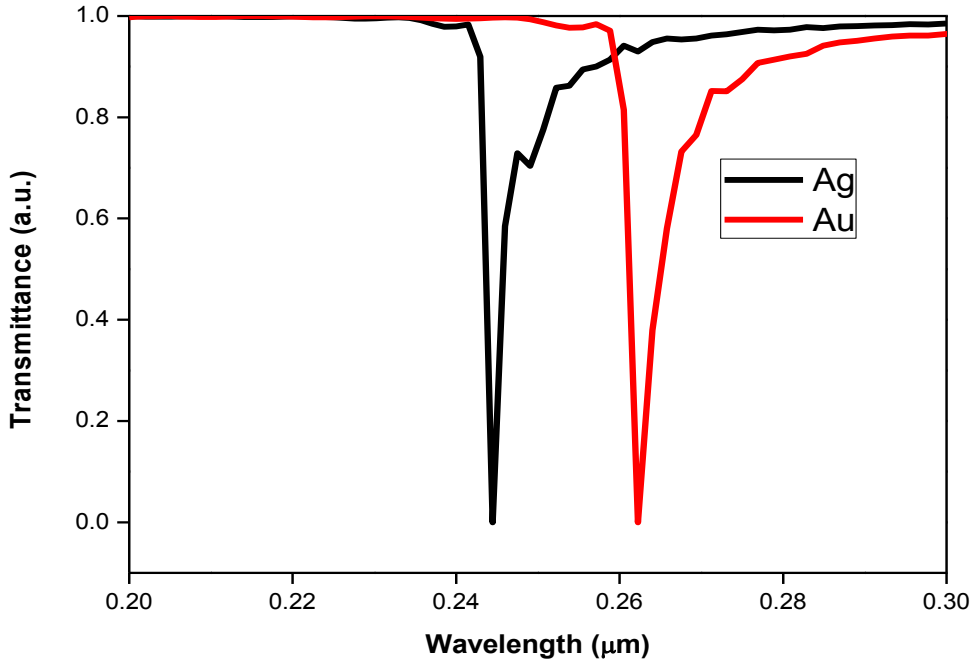

Fig.4.4 Transmittance curve of sensor for Ag and Au metal layers

To examine the effect of metal layer on sensor performance, we observed the features of (1) ITO-Ag-TiO_2 tri-layer SPR sensor (2) ITO-Au-TiO_2 based SPR sensor with same sensor parameters in fig 4.4. A narrower transmission curve for Ag based SPR sensor ($\Delta\lambda$ = 1.9 nm) in comparison to Au based SPR sensor ($\Delta\lambda$ = 2.2 nm) has been shown in above figure, i.e. DA is more with Ag metal based sensor (DA=0.55 nm^{-1}) in comparison to Au metal based sensor (DA=0.45 nm^{-1}).

4.4 CONCLUSION

The fiber optic sensor based on SPR with tri-layers of oxide-metal-oxide i.e. layers of ITO (internal layer) - Ag (center layer) - TiO_2 (an external layer) deposited on fiber core has been introduced. The proposed SPR sensor possesses high sensitivity, S_n = 17,807 nm-RIU^{-1} and fair accuracy of detection, DA = 526.3 μm^{-1}. We investigated that the minima in transmittance curve varies as a function of change in RI of sensing medium and also dependent on the thickness of the outer layer as well as on middle metal layer used in sensor structure. The benefits of the proposed SPR based FOS are miniaturization of the probe and its utilization in remote sensing applications that is not achievable with prism based SPR sensor.

CHAPTER 5

PERFORMANCE OF TRANSPARENT CONDUCTING METAL OXIDE-DEPOSITED SPR BASED OPTICAL FIBER REFRACTIVE INDEX SENSORS

Transparent Conducting Oxide (TCO)-deposited SPR based optical fiber sensors with Al:ZnO (AZO) and Ga:ZnO (GZO) having a film thickness of 18 nm coated on fiber core is presented and analysed theoretically and their suitability for a number of plasmonic applications is also discussed. The response curves and performance of these said sensors has been investigated in terms of sensitivity. The TCO deposited SPR based FOS with AZO and GZO have good response and high sensitivity as compared to conventional Au and Ag metal-deposited SPR sensors.

5.1 INTRODUCTION

SPR sensors are widely used in sensing applications as the SPs are highly sensitive to the change in the RI of the surroundings [39]. In SPR, when the p-polarised light having propagation constant equivalent to that of surface plasmon wave (an electromagnetic wave supported by metal-dielectric interface) is incident on M/D interface, a strong absorption of light occurs, hence SPR causes a decrease in the intensity of light reflected at specific angle or wavelength from the glass side of the sensor surface [16].

For sensing applications, many researchers used noble metal surfaces like silver (Ag)/ Gold (Au) to perform SPR because they show free electron behaviour as explained by free electron model. Masaru Mitsushio *et al.* [21] investigated the sensor properties and transmittance spectrums of Al-deposited SPR based FOS having film thickness of 7–70nm. Navneet K. Sharma *et al.* [25] theoretically and experimentally compared the response curves and performance of SPR sensor with Au, Ag, Cu and Al metal layers coated on the fiber-core, to anticipate the best possible metal for sensing applications.

In the near infrared region (NIR), the performance of plasmonic devices has been strictly constrained by large optical losses in noble metals [50,51]. An excess of research has been carried out to investigate the optical characteristics of different plasmonic materials like metal alloys, heavily doped semiconductors and transition-metal nitrides. It has been concluded that Al- and Ga-doped zinc oxide (AZO, GZO) and ITO are the common example of TCOs and are best alternatives over conventional metals as they show metallic behaviour, tunability and lesser material/optical loss with small magnitudes of real permittivity in comparison of Ag/Au in NIR. Carrier concentration higher than 10^{20} cm^{-3} is required for TCOs in order to exhibit plasmonic properties, which results in metal-like behaviour in NIR [52].

In this chapter, to improve the sensitivity of SPR sensor, Transparent Conducting Oxide (TCO)-deposited SPR based FOS has been presented. The FDTD method is used to simulate the said sensor for refractive index sensing and spectral interrogation method is utilised to examine the said sensor. Not only this structure has a good sensitivity but also overcomes the disadvantages of noble metal films.

This chapter is divided in four sections. In section 2, the theory and simulation setup for comparison of sensor performance with varying parameters, is discussed with component details. Section 3 deals with the detailed discussion of results observed after the simulation. Section 4 gives the conclusion of the dependence of sensor performance with varying refractive index.

5.2 THEORY AND SIMULATION SETUP

The principle of SPR sensing is attenuated total reflection (ATR) with Kretschmann's setup [12]. FOS based on SPR is presented with fiber core-TCO-sensing medium as shown in fig.5.1. As structure follows, cladding is firstly removed over the core (fiber core diameter = 20 μm and numerical aperture = 0.24) to firm up sensing region which is coated with thin TCO layer and further covered with sensing medium.

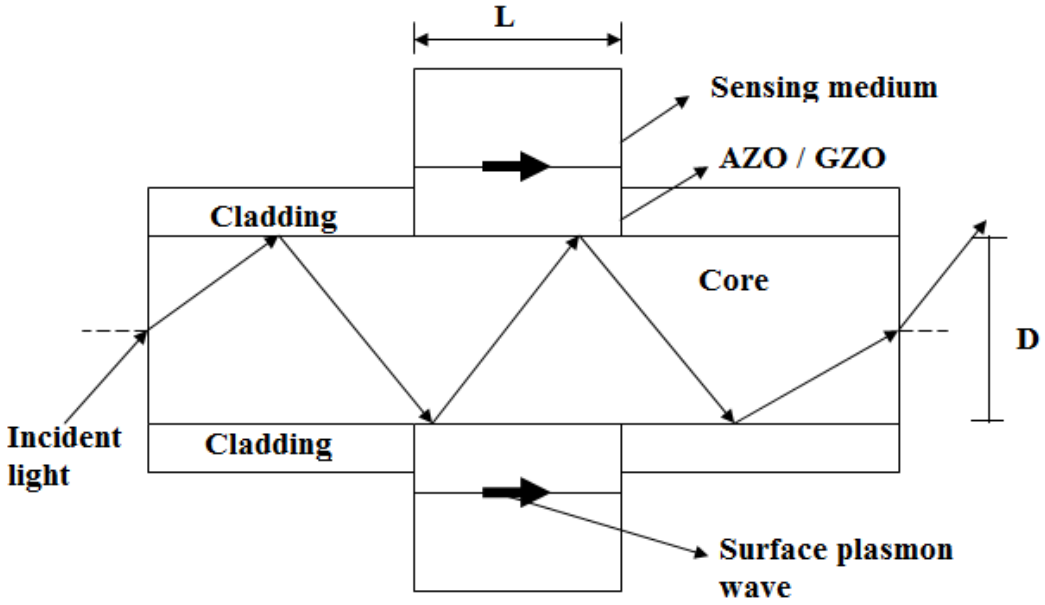

Fig.5.1. Layout of an optical fiber sensor based on SPR

Table 5.1: Parameters utilised for sensor:

Parameter	Numerical value
Fiber core diameter D	20 µm
Numerical aperture (NA)	0.24
Sensing region length L	100 µm

5.2.1 First Layer (Fiber core)

In fig.5.1, the fiber core is considered as first layer. According to Sellmeier dispersion equation, the RI of fused silica (n_1) varies with operating wavelength given as [36]:

$$n_1(\lambda) = \sqrt{1 + \frac{A_1\ \lambda^2}{\lambda^2 - B_1^2} + \frac{A_2\ \lambda^2}{\lambda^2 - B_2^2} + \frac{A_3\ \lambda^2}{\lambda^2 - B_3^2}} \qquad (5.1)$$

Where λ is the wavelength of incident light in µm with Sellmeier coefficients A_1 =0.6961663, A_2 =0.4079426, A_3 =0.8974794, B_1=0.0684043 µm, B_2= 0.1162414 µm, B_3= 9.896161 µm.

5.2.2 Second Layer (AZO/ GZO layer)

Second layer is prepared with TCOs and Drude-Lorentz oscillator model is utilized to calculate the dielectric constant of TCOs ($\in(\omega)$), which is (with all parameters listed in table 5.2), given as: [52,53]

$$\in(\omega) = \in_{\infty} - \frac{\omega_p^2}{\omega(\omega + i\Gamma_p)} + \frac{f_l \omega_l^2}{\omega_l^2 - \omega^2 - i\omega\Gamma_l} \tag{5.2}$$

Table: 5.2 Drude-Lorentz Model Parameters for AZO/GZO [52]

Parameters	**AZO (2wt%)**	**GZO (6wt%)**
Background permittivity ($\in_{\infty}$)	2.852	2.475
Unscreened plasma frequency (ω_p) (eV)	1.512	1.927
Carrier relaxation rate (Γ_p) (eV)	0.089	0.117
Strength of Lorentz oscillator (f_l)	0.596	0.866
Center frequency of Lorentz oscillator (ω_l) (eV)	4.384	4.850
Dampaing of Lorentz oscillator (Γ_l) (eV)	0.078	0.029

5.2.3 Third Layer (Sensing medium)

The TCO layer is surrounded with sensing medium, with dielectric constant $\in_s$, which is related to RI of sensing medium n_s as $\in_s = n_s^2$.

For the excitation of SPW, the resonance condition can be written as [15]:

$$\frac{2\pi}{\lambda} n_1 \sin\theta = Re\ \{K_{sp}\} \tag{5.3}$$

where $K_{sp} = \frac{w}{c}\sqrt{\frac{\epsilon(\omega)\epsilon_s}{\epsilon(\omega)+\epsilon_s}}$ is propagation constant of the SP, ω is frequency of incident light and c is speed of light in vacuum. Thus from the above equation a change in the RI of sensing medium can be calculated, by observing the shift in the resonance wavelength.

5.3 RESULTS AND DISCUSSION

In the previous sections, we discussed various components used in the simulation setup. Using this setup the measurement of magnitude of dip in response curve for both AZO and GZO has been performed. The result discussed below gives the comparison of response curves for both the considered cases.

Real and imaginary parts of spectral dielectric function can be calculated with the help of Drude-Lorentz equation and data given in table 5.2. Retrieved ϵ_{real} and ϵ_{img} parameters are listed in table 5.3.

Table 5.3: (a) Real part of dielectric constant (ϵ_{real})

Wavelength(μm)	AZO	GZO
0.9	2.5034	1.5958
1	2.1153	1.1052
1.1	1.6914	0.5693
1.2	1.2304	-0.0126
1.3	0.7317	-0.6403
1.4	0.1949	-1.3137
1.5	-0.3801	-2.0321

(b) Imaginary part of dielectric constant (ϵ_{img})

Wavelength(μm)	AZO	GZO
0.9	0.057	0.188
1	0.0758	0.2555
1.1	0.099	0.3379
1.2	0.127	0.4366
1.3	0.1602	0.5528
1.4	0.199	0.6879
1.5	0.2438	0.843

From the table 5.3(a) and (b), the optical properties of AZO and GZO can be graphically represented in fig.5.2 (a) and (b).

(a)

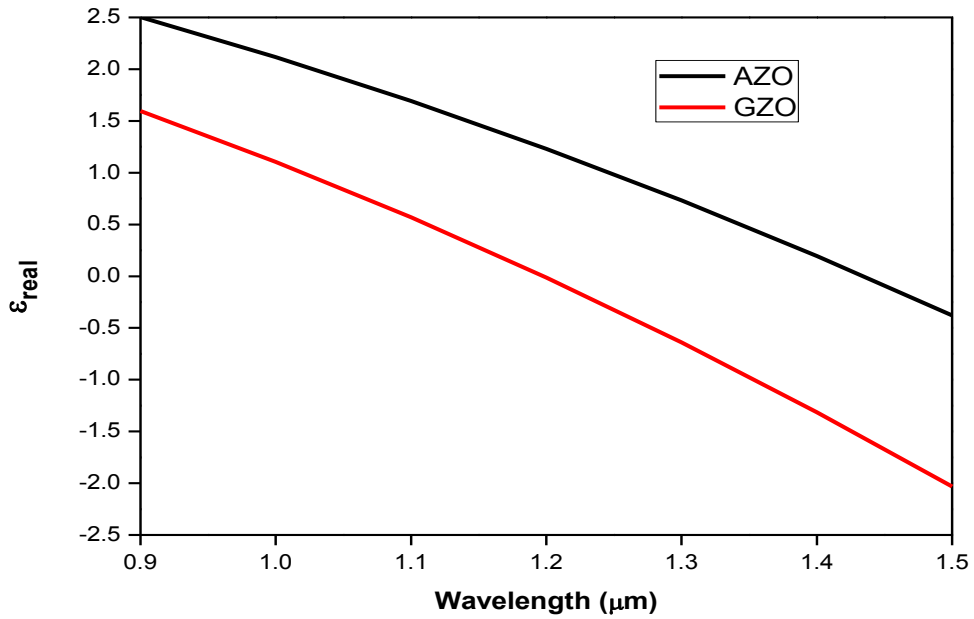

(b)

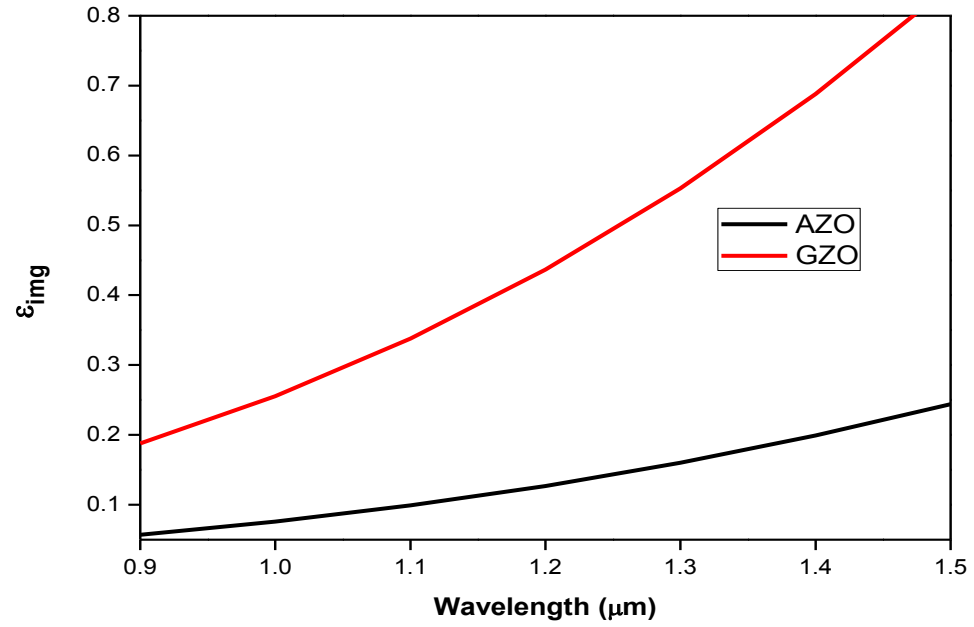

Fig.5.2 Comparison of (a) real and (b) imaginary part of dielectric constant of AZO and GZO

The optical properties (real and imaginary part of dielectric constant) of AZO and GZO films are shown in fig.5.2. The crossover wavelengths of all the TCO films are below telecommunication wavelength of 1.55 μm. As its imaginary part of permittivity of AZO is less, so it gives the smallest optical loss. However, in GZO the optical loss is greater than the AZO.

In SPR sensors the reflectance curve shows a minima at a specific wavelength; recognized as resonance wavelength (λ_{res}).A change in RI of sensing medium leads to change in λ_{res}, which is the basic concept of RI sensing. For AZO, the SPR sensor response was plotted as reflected power versus wavelength, as shown in fig.5.3 and we analysed that resonance wavelength is shifted towards the lower value with increase in the refractive index.

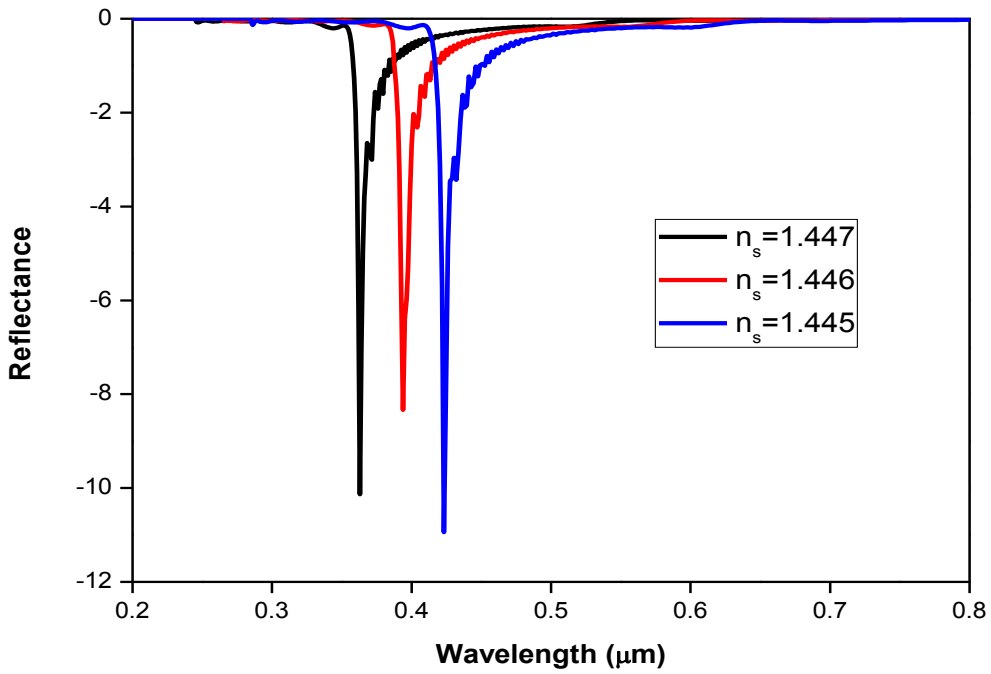

Fig.5.3 Shift in resonance wavelength in reflectance curve for AZO

The performance of a sensor is measured in terms of sensitivity (S_n). When the resonance wavelength is shifted by an amount $\delta\lambda_{res}$ with increase in RI of the sensing medium by δn_s then sensitivity of sensor is characterized as: $S_n = \frac{\delta\lambda_{res}}{\delta n_s}$. For estimating the sensor performance of said sensor, we calculated S_n = 30,240nm-RIU^{-1} from fig.5.3.

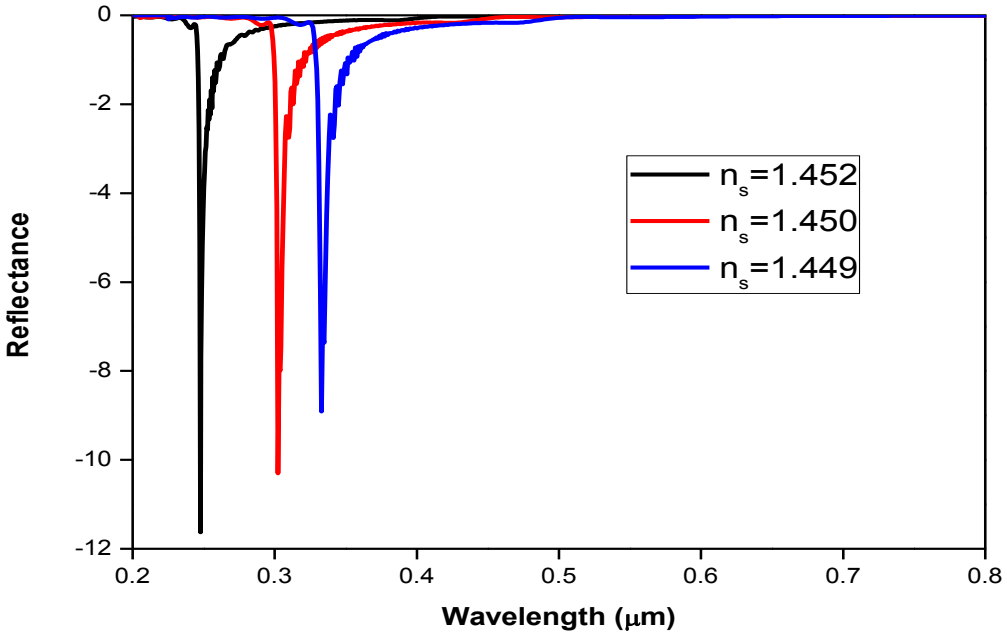

Fig.5.4 Shift in resonance wavelength of sensing curve for GZO

Fig.5.4 illustrates the plots of reflectance curve for GZO with respect to the resonance wavelength of SPR sensor for varying refractive indices of sensing medium i.e. 1.449, 1.450 and 1.452. The dips in the reflectance curve are occurring around 332.889 nm, 302.241 nm and 247.643 nm respectively for the varying RI of sensing medium.

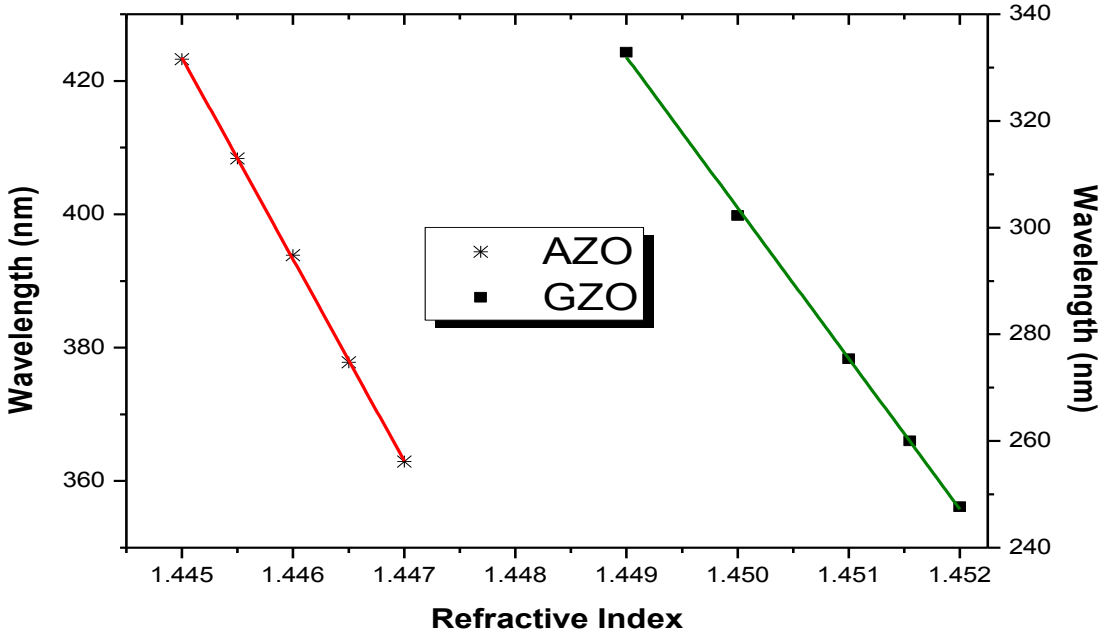

Fig.5.5. Wavelength shift versus refractive index graph for SPR sensor

A linear behaviour can be seen in the fig.5.5, that is the resonance wavelength of said sensor decreases linearly with increase in RI of sensing medium. The sensitivity (S_n) of the said sensor can be calculated by measuring the slope of the wavelength shift versus RI curve. Thus we achieved the sensitivities of AZO and GZO based SPR sensors are 30,240 nm-RIU^{-1}and 28,238 nm-RIU^{-1}.

5.4 CONCLUSION

The FOS based on SPR with TCOs layer i.e. layer of AZO / GZO coated on fiber core has been examined to determine the effect of TCO layer on SPR sensors. The investigated SPR sensor possesses higher sensitivity, S_n = 30,240 nm-RIU^{-1} for AZO and S_n = 28,238 nm-RIU^{-1} for GZO, in comparison to noble metal based SPR sensors. It is observed that the minima in reflectance curve, varies linearly as a function of change in refractive index of sensing medium. The benefits of the proposed SPR based fiber optic sensor are low intrinsic loss, semiconductor-based design, compatibility with standard nanofabrication processes, tunability etc. over the conventional metals based SPR sensors.

CHAPTER 6

CONCLUSION, RECOMMENDATIONS AND FUTURE SCOPE

6.1 CONCLUSION

This chapter presents the summary of investigation done in this dissertation. Firstly, conclusions are drawn from this research, after that the recommendations have been provided on the basis of the conclusions and further suggestions for future research are deliberated. The key results attained in this dissertation are summarized below:

1. The concept of modes for transmittance curve in SPR for different configurations has been presented. The various mode profiles are further investigated to examine the impact on the sensitivity of said sensor. All mode profiles for this sensor are studied using finite difference time domain simulations. Transmission spectra for different TM modes, are also compared for different operating wavelengths.
It has been observed that the thickness of metal film and operating wavelength are responsible for variation in the transmittance with respect to TM modes of the said sensor.

2. A FOS based on SPR with tri-layers of oxide-metal-oxide i.e. layers of ITO (internal layer) - Ag (center layer) - TiO_2 (an external layer) coated on fiber core has been presented. The proposed SPR sensor possesses high sensitivity, S_n = 17,807 nm-RIU^{-1} and fair accuracy of detection, DA = 526.3 μm^{-1}.

It has been also investigated that the minima in transmittance curve varies as a function of change in RI of sensing medium and is also dependent on the thickness of the outer layer as well as on middle metal layer used in sensor structure. The benefits of the proposed SPR based fiber optic sensor are miniaturization of the probe and its utilization in remote sensing applications that is not achievable with prism based SPR sensor.

3. The fiber optic sensor based on SPR with TCOs layer i.e. layer of AZO / GZO coated on fiber core has been examined to determine the its effect The investigated

SPR sensor possesses higher sensitivity, S_n = 30,240 nm-RIU^{-1} for AZO and S_n = 28,238 nm-RIU^{-1} for GZO, in comparison to noble metal based SPR sensors. It is observed that the minima in reflectance curve, varies linearly as a function of change in RI of sensing medium. The benefits of the proposed SPR based fiber optic sensor are low intrinsic loss, semiconductor-based design, compatibility with standard nanofabrication processes, tunability etc. over the conventional metals based SPR sensors.

6.2 RECOMMENDATIONS

1. The selection of optimized thickness of metal film and operating wavelength is recommended, as both are responsible for variation in the transmittance curve with respect to TM modes of the fiber optic based SPR sensor.

2. The use of ITO-Ag-TiO_2 tri-layer SPR sensor over Bi-layer based SPR sensor is preferred as the former offers the high sensitivity and fair accuracy of detection i.e. it provides enhanced results.

3. It is recommended to use TCOs coated fiber optic SPR sensor in place of conventional metal films coated fiber core.

6.3 FUTURE SCOPE

SPR based FOS are bound to encounter more advancement in future, especially in bio sensors, nano sensors, and photonic crystal based SPR sensors. SPR sensors have to compete with existing technologies on the basis of multiple factors such as robustness, low cost, stability, ease of use and sensitivity. It is predicted that this will drive research and development of SPR-sensing devices in the following directions:

1. Improvement of detection limit: Further optimization of SPR optical instruments and development of efficient referencing concepts and sophisticated data processing methods may improve the resolution of SPR-sensing devices.

2. Though copper deposited optical fiber sensors shows good properties but the protection of the copper film from oxidation and corrosion is a major parameter which needs to be researched more for stable use of this type of sensor.

3. Photonic crystal fiber (PCF)-based SPR sensors are bound to find new heights in the coming future due to their unique optical properties such as omni-directionality, negative refractive indices and gapless guidance.

4. For further optimization of crucial factors and parameters to improve the sensor performance, following steps can be used, like

- New combinations such as metal-semiconductor nano-composite, different bimetallic alloys (with nano particles of different metals such as Cu, Au, Ag, and Al) are to be utilized in SPR based FOS.
- The collaboration of fiber grating and LSPR technique is another candidate for further research in this area.

Undoubtedly, in the future, the SPR technology will be benefited from the use of optical waveguide technology which offers the potential for development of miniaturized, compact, and rugged sensing elements with prospect of fabrication of multiple sensors on one chip. Thus there is plenty of room to work with these sensors and it will surely benefit us for so many purposes.

REFERENCES

[1] F. T. S. Yu and S. Yin, Fiber Optic Sensors, New York: CRC Press, 2002.

[2] D. A. Krohn, Fiber Optic Sensors: Fundamentals and Applications, Research Triangle, NC: ISA, 1988.

[3] B. Culshaw, "Fiber optics in sensing and measurement," *IEEE Journal of Selected Topics in Quantum Electronics,* vol. 6, no. 6, pp. 1014-1021, 2000.

[4] P. M. Tracey, "Intrinsic fiber optic sensors," *IEEE Transactions on Industry Applications,* vol. 27, no. 1, pp. 96-98, 1991.

[5] J. Homola, S. S. Yee and G. Gauglitz, "Surface plasmon resonance sensors: review," *Sensors and Actuators B,* vol. 54, no. 1-2, pp. 3-15, 1999.

[6] C. Nylander, B. Liedberg and T. Lind, "Gas detection by means of surface plasmon resonance," *Sensors and Actuators,* vol. 3, no. 1, pp. 79-88, 1982.

[7] R. W. Wood, "On a remarkable case of uneven distribution of light in a diffraction grating spectrum," *Philosophical Magazine,* vol. 4, no. 1, pp. 396-402, 1902.

[8] J. Zenneck, "Uber die fortpflanztmg ebner elektro-magnetischer wellen langs einer ebenen leiterflache and ihre beziehung zur drahtlosen telegraphie," *Annalen der Physik,* vol. 328, pp. 846-866, 1907.

[9] A. Sommerfeld, "Propagation of waves in wireless telegraphy," *Anals der Physik,* vol. 28, pp. 665-736, 1909.

[10] R. H. Ritchie, "Plasma losses by fast electrons in thin films," *Physical Review,* vol. 106, no. 5, pp. 874-881, 1957.

[11] A. Otto, "Excitation of nonradiative surface plasma waves in silver by the method of frusted total reflection," *Zeitschrift für Physik,* vol. 216, no. 4, pp. 398-410, 1968.

[12] E. Kretschmann and H. Reather, "Radiative decay of non-radiative surface plasmons excited by light," *Zeitschrift für Naturforschung,* vol. 23A, pp. 2135-2136, 1968.

[13] N. D. Lang and W. Kohn, "Surface dipole barriers in simple metals," *Physical Review B,* vol. 8, no. 12, pp. 6010-6012, 1973.

[14] H. Raether, Surface plasmons on smooth and rough surfaces and on gratings, Springer, Verlag, 1988.

[15] A. K. Sharma, R. Jha and B. D. Gupta, "Fiber- optic sensor based on surface plasmon resonance: a comprehensive review," *IEEE Sensors Journal,* vol. 7, no. 8, pp. 1118-1129, 2007.

[16] B. D. Gupta and R. K. Verma, "Review article surface plasmon resonance- based fiber optic sensors: principle, probe design and some applications," *Journal of Sensors,* vol. 2009, pp. 1-12, 2009.

[17] A. K. Sharma and B. D. Gupta, "Fiber optic sensor based on surface plasmon resonance with Ag-Au alloy nanoparticles films," *Nanotechnology,* vol. 17, pp. 124-131, 2006.

[18] A. K. Mishra, S. K. Mishra and B. D. Gupta, "SPR based fiber optic sensor for refractive index sensing with enhanced detection accuracy and figure of merit in visible region," *Optics Communications,* vol. 344, pp. 86-91, 2015.

[19] M. Mitsushio, K. Miyashita and M. Higo, "Sensor properties and surface characterization of the metal-deposited SPR optical fiber sensors with Au, Ag, Cu, and Al," *Sensors and Actuators A,* vol. 125, no. 1, pp. 296-303, 2006.

[20] R. K. Verma, A. K. Sharma and B. D. Gupta, "Surface plasmon resonance based tapered fiber optic sensor with different taper profiles," *Optics Communications ,* vol. 281, no. 6, pp. 1486–1491, 2008.

[21] M. Mitsushioa, K. Watanabeb, Y. Abeb and M. Higoa, "Sensor properties and surface characterization of aluminum-deposited SPR optical fibers," *Sensors and Actuators A: Physical,* vol. 163, no. 1, pp. 1-8, 2010.

[22] T. Woo-Hu, L. Yu-Cheng, T. Jiu-Kai and T. Yu-Chia, "Multi-step structure of side-polished fiber sensor to enhance SPR effect," *Optics & Laser Technology,* vol. 42, no. 3, pp. 453-456, 2010.

[23] S. Singh, R. K. Verma and B. D. Gupta, "LED based fiber optic surface plasmon resonance sensor," *Optical and Quantum Electronics,* vol. 42, no. 1, pp. 15-28, 2010.

[24] T. Srivastava, R. Jha and R. Das, "High-performance bimetallic SPR sensor based on periodic-multilayer-waveguides," *IEEE Photonics Technology Letters,* vol. 23, no. 20, pp. 1448-1450, 2011.

[25] N. K. Sharma, "Performances of different metals in optical fiber-based surface plasmon resonance sensor," *Pramana journal of physics,* vol. 78, no. 3, pp. 417-427, 2012.

[26] K. Sathiyamoorthy, B. Ramya, V. M. Murukeshan and X. Wei Sun, "Modified two prism SPR sensor configurations to improve the sensitivity of measurement," *Sensors and Actuators A* , vol. 191, no. 1, pp. 73-77, 2013.

[27] N. K. Sharma, M. Rani and V. Sajal, "Surface plasmon resonance based fiber optic sensor with double resonance dips," *Sensors and Actuators B* , vol. 188, no. 1, pp. 326– 333, 2013.

[28] H. Tu, T. Sun and K. T. Grattan, "SPR-based optical fiber sensors using gold–silver alloy particles as the active sensing material," *IEEE Sensors Journal,* vol. 13, no. 6, pp. 2192-2199, 2013.

[29] P. Bhatia and B. D. Gupta, "Surface plasmon resonance based fiber optic refractive index sensor utilizing silicon layer: effect of doping," *Optics Communications,* vol. 286, no. 1, pp. 171–175, 2013.

[30] Y. Al-Qazwini, A. S. M. Noor, T. K. Yadav, M. H. Yaacob, S. W. Harun and M. A. Mahdi, "Performance evaluation of a bilayer SPR-based fiber optic RI sensor with TiO_2 using FDTD solutions," *Photonic Sensors,* vol. 4, no. 4, pp. 289–294, 2014.

[31] W. Hu Tsai, K. Cherng Lin, S. Ming Yang, Y. Chia Tsao and P. Jing Ho, "Fiber-optic surface plasmon resonance-based sensor with AZO/Au bilayered sensing layer," *Chinese Optics Letters*, vol. 12, no. 4, pp. 1-3, 2014.

[32] H. Moayyed, I. T. Leite, L. Coelho, J. L. Santos and D. Viegas, "Theoretical study of phase-interrogated surface plasmon resonance based on optical fiber sensors with metallic and oxide layers," *Plasmonics* , vol. 9889, no. 2, pp. 1-9, 2015.

[33] S. Lee and K. Kim, "Analytical determination of multilayer waveguide modes," *Journal of the Korean Physical Society*, vol. 51, no. 1, pp. 104-106, 2007.

[34] G. Griffel, S. Ruschin and N. Croitoru., "General approach for calculating the number of modes in graded index waveguides," *Journal of the Optical Society of America A* , vol. 4, no. 7, pp. 1296-1303 , 1987.

[35] J. W. Y. Lit, Y. F. Li and D. W. Hewak, "Guiding properties of multilayer dielectric planar waveguides," *Canadian Journal of Physics*, vol. 66, no. 10, pp. 914-940, 1988.

[36] A. K. Ghatak and K. Thyagarajan, An introduction to fiber optics, Cambridge, UK: Cambridge University Press, 1999.

[37] M. A. Ordal, L. L. Long, R. J. Bell, S. E. Bell, R. R. Bell, R. W. Alexander Jr and C. A. Ward, "Optical properties of metals Al, Co, Cu, Au, Fe, Pb, Ni, Pd, Pt, Ag, Ti, and W in the infrared and far infrared," *Applied Optics*, vol. 22, no. 7, pp. 1099-1119, 1983.

[38] H. Kogelnik, "Theory of Optical Waveguides," Springer Berlin Heidelberg, 1988, pp. 7-88.

[39] R. Slavik, J. Homola and J. Ctyroky, "Miniaturization of fiber optic surface plasmon resonance sensor," *Sensors and Actuators B*, vol. 51, no. 1, pp. 311–315, 1998.

[40] B. D. Gupta and A. K. Sharma, "Sensitivity evaluation of a multi-layered surface plasmon resonance-based fiber optic sensor: a theoretical study," *Sensors and*

Actuators B: Chemical, vol. 107, no. 1, pp. 40-46, 2005.

[41] C. Rhodes, S. Franzen, J. P. Maria, M. Losego, D. N. Leonard, B. Laughlin, G. Duscher and S. Weibel, "Surface plasmon resonance in conducting metal oxides," *Journal of Applied Physics,* vol. 100, no. 5, pp. 1-4, 2006.

[42] C. Rhodes, M. Cerruti, A. Efremenko, M. Losego, D. E. Aspnes, J. P. Maria and S. Franzen, "Dependence of plasmon polaritons on the thickness of indium tin oxide thin films," *Journal of Applied Physics,* vol. 103, no. 9, pp. 1-6, 2008.

[43] J. T. Guske, J. Brown, A. Welsh and S. Franzen, "Infrared surface plasmon resonance of AZO-Ag-AZO sandwich thin films," *Optics Express* , vol. 20, no. 21, pp. 23215-23226, 2012.

[44] S. H. Brewer and S. Franzen, "Calculation of the electronic and optical properties of indium tin oxide by density functional theory," *Chemical Physics,* vol. 300, no. 1, pp. 285-293, 2004.

[45] I. D. Villar, C. R. Zamarreno, M. Hernaez, F. J. Arregui and I. R. Matias, "Lossy mode resonance generation with indium tin oxide coated optical fibers for sensing applications," *Journal of Lightwave Technology,* vol. 28, no. 1, pp. 111-117, 2010.

[46] W. H. Weber and S. L. Mccarthy, "Surface-plasmon resonance as a sensitive optical probe of metal-film properties," *Physical Review B,* vol. 12, no. 12, pp. 5643–5650, 1975.

[47] D. Ciprian and P. Hlubina, "Simulation of surface plasmon fiber-optic sensor including the effect of oxide overlayer thickness change," *in Proc. SPIE,* vol. 8439, no. 1, pp. 1-11, 2012.

[48] N. Díaz-Herrera, A. González-Cano, D. Viegas, J. L. Santos and M. C. Navarrete, "Refractive index sensing of aqueous media based on plasmonic resonance in tapered optical fibres operating in the 1.5 μm region," *Sensors and Actuators B: Chemical,* vol. 146, no. 1, pp. 195-198, 2010.

[49] S. Singh and B. D. Gupta, "Simulation of a surface plasmon resonance-based

fiber-optic sensor for gas sensing in visible range using films of nanocomposites," *Measurement Science and Technology,* vol. 21, no. 11, pp. 1-8, 2010.

[50] P. R. West, S. Ishii, G. V. Naik, N. K. Emani, V. M. Shalaev and A. Boltasseva, "Searching for better plasmonic materials," *Laser & Photonics Reviews ,* vol. 4, no. 6, pp. 795-808, 2010.

[51] A. Boltasseva and H. A. Atwater, "Low-loss plasmonic metamaterials," *Science,* vol. 331, no. 6015, pp. 290–291, 2011.

[52] J. Kim, G. V. Naik, N. K. Emani, U. Guler and A. Boltasseva, "Plasmonic resonances in nanostructured transparent conducting oxide films," *IEEE Journal of Selected Topics in Quantum Electronics,* vol. 19, no. 3, pp. 1-7, 2013.

[53] G. V. Naik, V. M. Shalaev and A. Boltasseva, "Alternative plasmonic materials: beyond gold and silver," *Advanced Materials,* vol. 25, no. 24, pp. 3264-3294, 2013.

LIST OF PUBLICATIONS

[1] Pragya, R. S. Kaler, "Effect of different TM modes on the sensitivity of Surface Plasmon Resonance based optical fiber sensor" communicated to Optoelectronics and Advanced Materials - Rapid Communications (OAM-RC).

[2] Pragya, R. S. Kaler, "Wavelength Interrogated Fiber Optic Sensor Based on Surface Plasmon Resonance with Oxide-Metal-Oxide layers using FDTD Solutions" communicated to Fiber and Integrated Optics Journal.

[3] Pragya, R. S. Kaler, "Performance of Transparent Conducting Metal Oxide-deposited SPR based Optical Fiber Refractive Index Sensors" communicated to Optik- International journal for light and electron.

[4] Pragya, Shailly Khanna, R. S. Kaler, "Photonic Crystal Fiber Plasmonic Sensor Based on Bi-Coated Microfluidic Channels" published in International conference on Electrical, Electronics, Computer Science and Mathematics Physical Education and Management (ICEECMPE) in New Delhi.

.